From disorder to order as applied to the movement of micro-organisms

G. R. Ivanitskiĭ, A. B. Medvinskiĭ, and M. A. Tsyganov

Institute of Biological Physics, Academy of Sciences of the USSR, Pushchino, Moscow Province

(Submitted November 22, 1990)
Usp. Fiz. Nauk **161**, 13–71 (April 1991)

This review is devoted to an investigation of the pattern formation problem in mobile micro-organism populations. This pattern formation is due to the nonlinear character of the processes which control the behavior of an individual organism. Various examples of the pattern formation (population waves, swarms, Rayleigh–Taylor cells, "green holes", etc.) are reviewed in detail. It is demonstrated that the stability of these patterns is due to the interaction between organism and environment. The importance of investigating the transformation from random motion of individual cells to determinate behavior of cellular collectives for progress in bioengineering is discussed.

1. STATEMENT OF PROBLEM

The question—how is chaos in various systems of nature spontaneously transformed into order?—is one of the fundamental questions in physics and biophysics. Its answer, as it seems to us, must be based not on a postulation of the special properties of time,[1] but on a study of the general laws governing self-consistency and inconsistency of cyclical processes at various levels of structural organization of matter.

It would seem intuitively clear that disorder cannot transform itself into order and, consequently, we cannot assure ourselves of the state of nonliving and living matter, which we observe around us, by a brute-force exhaustive search. Banal statements, applied to evolutionary processes, that a pile of stones cannot compose itself, for example, into the Mother of God Cathedral in Paris or that the novel "War and Peace" will never be written by a random search through the letters of the alphabet are repeated many times in various publications. Nevertheless, the evolution of living and nonliving matter gives many examples that contradict these statements. Consequently, there is a gap in our knowledge which prevents us from comprehending a unified picture of the world.

Block-hierarchical principles of exhaustive search show that the time necessary for the selection of patterns that are stable to outside conditions can be reduced by several orders of magnitude through a parallel exhaustive search by blocks.[2] However, in order to understand the search mechanism we need an answer to the following questions: What local properties must be imparted to various pattern levels of the block element, self-selected into the whole of the following level? How did these properties appear? To what diverse consequences can interactions of these elements lead?

It is necessary to find a compromise between the following thesis and anti-thesis: "The medium controls the object—the object shapes the medium", namely, to place the connective "and" between them rather than the separating word "or". In other words, to close them—via feedback—in the pattern level within the cycle that has been chosen for study.

By observing various physical and biological systems, one can see the hierarchy of the "object $\rightleftarrows$ external medium" cycles and the hierarchy of the memory "devices", ensuring the stability and mutability of the systems. Such devices have different times to remember and to realize the stored information. The renewal rate of blood—the most responsive element of the human organism—is 15×10^7 erythrocytes/min, 2×10^5 leucocytes/min, and 2.5×10^8 thrombocytes/min; the renewal rate of protein mycelia is even higher. On the other hand, as is known, nerve tissue is not renewed structurally: neurons essentially do not multiply. Their lifetime is the life of the human, but if one considers the neuron content at another pattern level—internal biochemical metabolism—then one can witness extremely rapid changes.

We also observe cyclicity of the organization of processes at the molecular level. Whereas before the 1970s it was assumed that the genomes of organisms are stable, now it is necessary to speak of a dynamic stability: a state that is stable in some external conditions may be unstable in others.[3] In DNA mobile genes have been observed—regions capable of moving under the influence of a change in the ambient from point to point in the genome of any biological systems—from bacteria to man. The structure of such jumping regions can contain one or several genes. It has turned out that such jumping genes are rather large in number. It is possible that they provide for the mechanism of the second level of genetic mutations, playing an important role in accelerating biological evolution processes and the adaptability of living organisms to the surrounding medium, in contrast to the first level-point mutations. Thus, in addition to the long-known bisexual variant in nature, which accelerates the adaptation of living organisms to environmental changes, there are many other methods for the disordering and assembly of genetic material.

In biology and demography, interchanges of generations are an interesting type of cycle, and the spatial wave patterns produced by them are also of interest. Such waves show up most clearly in time during the multiplication of a synchronous culture of micro-organisms in a fermenter, and in space during the transfer of cultures of plants or animals from one region to another or during the development of new territories by a population of people originally close in age, etc.[4] The cyclical character of the multiplication of living organisms lies, on the one hand, at the base of the mechanism for the appearance of waves (for example, the division cycle for various micro-organisms lasts 0.5–2 hours, for various human cells it is 10–100 hours, and the reproductive period of a human population synchronous in time is 25–27

 0038-5670/91/040289-28$01.00

years). On the other hand, outside conditions exert a significant influence on the shape and evolution of the space-time patterns formed in this case.

In order to analyze processes that are similar but extremely specific in nature, it is important to choose a subject for experimental investigation that would correspond both to the simplicity of its transformation and also to fast pattern metamorphoses (on the time scale of human life)—in order to be able, within a comparatively short length of time, to draw conclusions about mechanisms of self-organization and about the influence of the ambient on their space-time characteristics. A fortuitous choice of test object may make it possible to come close to an understanding of the general regularities of behavior and may be able to give answers to the questions posed above. These considerations caused us to turn to the world of bacteria.

Of course, analogies are not the most reliable way of understanding nature. The only advantage is that in the search for answers to the global questions posed above through a study of micro-organisms we are also solving practical problems at the same time. It is well known that knowledge about the behavior of bacteria is important not only for biology and medicine, but also for bioengineering[5] and biotechnology.[6] Table I gives some examples of the use of micro-organisms in biotechnology.

Let us point out that the results presented below by no means claim to be a general theory of synergism and in no case can they replace the study of other real systems; it is our belief, rather, that they can only supply, on the basis of analogies and mathematical modeling, additional information and new ideas necessary for investigating other nonbacterial systems.

Anyone can see that individual bacteria move chaotically. To do so it is sufficient to peer into a microscope at a drop of a culture medium inoculated beforehand, for example, with colon bacillus [Latin name—*Escherichia (E.) coli*]. Using a sophisticated experimental technique, Berg was able to demonstrate this quite rigorously.[7,8]

Moreover, it is known that chaotically moving bacteria can under certain conditions be distributed nonuniformly in space, i.e., they can form spatial patterns that both vary with time and remain unchanged (see, e.g., Ref. 9).

It is usually assumed that the appearance of such patterns or self-organization in a system of chaotically moving organisms is governed not by biological laws but by fundamental physical laws.[10] Namely, the appearance of order in the system can be caused both by its remoteness from thermodynamic equilibrium, and also by the nonlinearity of its characteristics.[11] What are the mechanisms for the specific realization of these physical laws during pattern formation

TABLE I. Some biotechnological products and their producers.

Products	Producers	Products	Producers
Microbe proteins:		L-lysine, 5′-inosine and 5′-guanyl acids	Corynebacterium glutamicum
From paper wastes	Candida utilis		
From aliphatic petroleum hydrocarbons	Saccharomycopsis lipolytica		
From methane or methanol	Methylophilus, methylotrophus	Medicinal preparations, penicillin	Penicillum
		Cephalosporins	Cephalosporium acremonium
Enzymes:		Amphotericin B, kanamycins, neomycins, streptomycin, tetracyclines, etc.	Streptomyces
Amylases	Aspergillus oryzae		
Glucoamylase	Aspergillus niger		
Cellulase	Trichoderma reesii		
Invertase	Saccharomyces cerevisiae	Gramacidin S [S-Soviet]	Bacillus brevis
Lactase	Kluyveromyces fragilis	Bacitracin	Bacillud subtilis
Lipase	Saccharomycopsis lipotytica	Polymyxin B	Bacillus polymyxa
			Rhizopus nigricans
Vitamins:		Steroid modifications	Arthrobacter simplex
Riboflavin	Eremothecium ashbyi		Mycobacterium
Vitamin B_{12}	Pseudomonas denitrificans	Immunoglobulins and monoclonal antibodies	Hybridomes (obtained by cell engineering methods)
Polysaccharides:			
Dextran	Leuconostoc mesentroides		
Xanthic resin	Xanthomonas campestris	Interferon	Lines of mammalian cells (obtained by cell engineering methods)
Carotenoids			
Beta-carotene	Blakeslea trispora		
Astaxanthin	Phaffia rhodozyma		
Amino acids and derivatives of nucleotides		Insulin, human growth hormone, somatostatin interferon	Escherichia col. (recombination DNA by gene engineering methods)

FIG. 1. *Salmonella typhimurium* bacteria during free steady swimming.[117]

in populations of mobile bacteria? This review is an attempt to answer this question, which is not only specific, but is also directly related to the general issues raised above.

2. LAWS OF MOTION FOR AN INDIVIDUAL BACTERIUM

2.1. Some features of this motion

By the end of the 19th century Cohn, Engelmann, and Pfeffer[32-36] had showed that bacteria in a culture medium are able to change their direction of motion, in some cases, avoiding company and in other cases striving to mingle. However, a systematic investigation of the mobility and behavior of bacteria was begun only quite recently, and considerable successes have been achieved in this area during the past 20 years.

A distinguishing characteristic of many bacteria is the presence of special mobile organella—filaments—on them. Peritrichous bacteria, having filaments randomly spread over the entire surface of a body (these include the *E. coli, Salmonella (S.) typhimurium, Bacillus*, etc. bacteria; Fig. 1), actively move about, alternating periods of steady directional swimming (or free drift) with periods of so-called tumbling. In the tumbling state the cells lose their orientation and perform abrupt chaotic motions, resembling a tremor and somersaulting. The periods of steady swimming usually amount to 1–4 sec while the tumbling is about 0.1 sec in duration (Fig. 2).[8,14,37] In order to demonstrate such a type of motion, Berg, from Harvard University, set up experimentally a "Lagrangian coordinate system". He built an automated microscope, capable of tracking the motion of an individual cell in three dimensions (Fig. 3).[7,8]

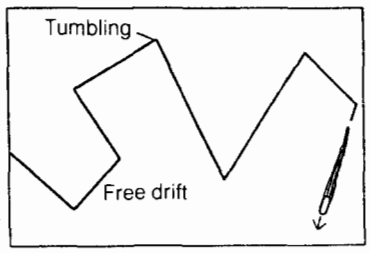

FIG. 2. Random walk, typical of the *Escherichia coli* bacteria.[116]

In this microscope the image of the bacterium was focused onto the ends of six optical fibers, each of which was connected to a photomultiplier. The fibers were mounted pairwise. One pair tracked to the right and left sides of the image, another to its front and back sides, while the third pair of fibers tracked the upper and lower parts of the image (above and below the focal plane). The signal difference from each pair was amplified and was used to control the geometrical position of the small chamber with the bacterium swimming in it; the chamber was placed inside an electromechanical transducer. With the movement of the bacterium, located at the focus of the microscope, the chamber was displaced in the direction in which the amplitude of the difference signals decreased; in this way the image of the bacterium was always at the center of the microscope field of view. Thus, the coordinate of the cell in the laboratory reference system did not change, and its motion was inferred from the displacement of the chamber in which it was swimming.

It turned out that the tumbling frequency for fixed ambient conditions does not change with time. After each tum-

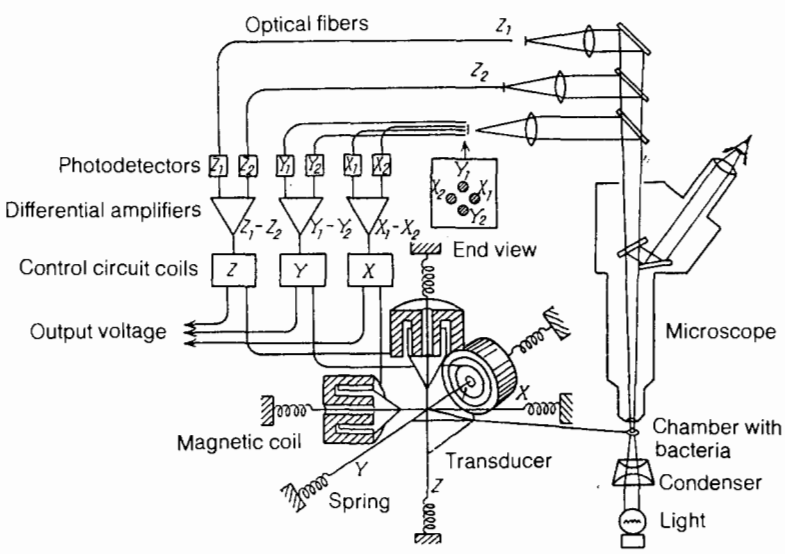

FIG. 3. Automated system for tracking the motion of an individual bacterium.[8]

bling the direction of motion changes in a random fashion.[8,14]

As already pointed out, directional motion of many bacteria is provided by filaments (or flagella). The filaments, being the motive apparatus of bacteria, rotate, interweaving themselves into a helical bundle behind the cell body (Fig. 1). A hydrodynamic force is created in this situation, pushing the cell forward.[8,38]

2.2. Mechanics of micro-organism motion

In examining moving bacteria the investigator is justified in being interested in the question: what are the laws of this motion? It turns out that bacteria in their "everyday life" adhere to Aristotelian mechanics rather than Newtonian. In other words, their motion (between tumblings) is completely determined by the velocity at a given moment and does not depend on the changes in velocity in preceding moments.[12] In fact, for microorganisms (with a characteristic size of $\sim 1\mu$m) the values of the Reynolds number (Re) are many orders of magnitude smaller than in the world familiar to us, being[13] about 10^{-4}. It is easy to show that for such Re values the path, traversed by a micro-object by virtue of inertia, amounts to ~ 0.1 Å, and the slowing time (from an initial velocity of $20\,\mu$m/sec, typical for bacteria,[14] to a complete standstill) is about $0.3\,\mu$sec. It is only during this time interval (so small!) when the bacterium is moving by virtue of inertia that it "remembers" how it was moving earlier.

It is interesting that the dependence of the velocity U of the cell on the viscosity of the culture medium is not monotonic:[40,41] with a decrease in the viscosity the value of U starts to increase sharply, but then it gradually decreases. What does this mean? It was shown[42] that

$$U = (E/D)^{1/2}\,(d\omega/dt)^{1/2}, \qquad (1)$$

where E is the efficiency of the motor, D is the drag of the medium (for spherical objects of radius A and for $\mathrm{Re} \ll 1$ the result is $D = 6\pi\mu A$, where μ is the dynamic viscosity), and $d\omega/dt$ is the power expended by the organism in the process of moving in a viscous medium. According to Eq. (1) the increase of U with an increase in viscosity can be explained by an increase in E and (or) by an increase in $d\omega/dt$. There are grounds for assuming[41] that the velocity of bacteria depends primarily on their efficiency (E in Eq. (1)). In turn, the quantity E depends on the geometrical parameters of the spatial helix formed by the flagella during the directional motion of bacteria (see Fig. 1).[43,44] This means that the velocity U must change because of conformational changes in the bacterial filaments. Experiments have confirmed this fact.[41] The conformation of the filaments, however, depends on the Reynolds number.[45,46] Thus, the viscosity of the medium controls the conformation of the flagellar helical wave, namely, its amplitude n and wave number k. According to Ref. 43, the value of E increases with an increase in viscosity, reaches a maximum at $nk = 1$, and then decreases. In accordance with Eq. (1) the velocity U also varies in a similar fashion. Thus, the velocity of bacteria depends not only on the properties of the medium but also on the parameter E, also characterizing the internal processes occurring in the cells and providing for their vital activity.

The motion of bacteria for $\mathrm{Re} \ll 1$ requires constant expenditures of energy to maintain the motion (even with a constant velocity—in complete accordance with Aristotelian physics). The source of this energy is the electrochemical proton gradient ($\Delta\bar{\mu}_{H^+}$), applied across the membrane separating the internal medium of the bacterium from the surrounding medium.[15–20] The energy stored up in this fashion is expended in the wavy motion of the bacterial flagella (or filaments). The flagella, interwoven into a bundle, form a left-handed helix (see, e.g., Ref. 47). When this bundle rotates counterclockwise along its length (from the proximal to the distal part), a wave propagates. During the interaction of the wave with the viscous liquid, as already indicated above, forces arise pushing the cell forward.[8,38]

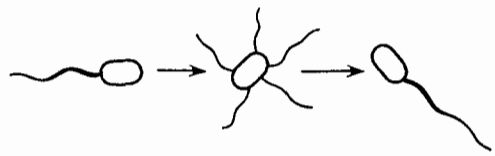

FIG. 4. Change in direction of motion of bacterium as a result of tumbling caused by untwisting of filament.[84]

The other mode of bacterial movement—tumbling—arises when the bundle of filaments starts to rotate clockwise.[47–50] In this situation the bundle unwinds (Fig. 4) and the directional motion of the bacterium ceases; it is replaced by a random change in cell orientation.

Nonperitrichial organisms use other principles to change direction.[27,38,51] For example, the bipolar *Rhodospirillum rubrum* or *Spirillum volutans* bacteria have two bundles of flagella, located at opposite poles. The leading strand bends backward and rotates around the body of the cell; the other strand is a continuation of the cell and rotates about its axis. The strands change rotation direction and orientation with respect to the cell periodically, causing a reversal in its motion.[51,52] The front strand causes translational motion, rotating the cell; the cell, being a helix,[21] is "screwed into" the culture medium. The hydrodynamic laws of this motion have been investigated.[42,44,53]

2.3. Mechanism and operating principle of the motor of bacteria

According to electron microscope data the filaments consist of three basic parts: the basal body, located within the cell wall, the hamulus, and the outer helical thread associated with it, which plays the role of a screw for the motion of the bacteria (Fig. 5).[22–24] The basal body in turn consists of four rings, a rod passing through their centers, as well as a cylinder connecting the two distal rings (see Fig. 5). It has been shown that the individual rings, visible within the field of view of an electron microscope, have a 16-fold symmetry axis. It may be that each ring is constructed from 16 protein subunits.

The basal body is connected to the thread of the flagella by the hamulus having a length of about 90 nm (see Fig. 5). The thread of the bacterial filament is a helical protein formation with a length up to $20\,\mu$m and a diameter of 12–20 nm. The pitch of the helix[25–27] is about $2.5\,\mu$m. It is assumed that the hydrophobic bonds[28,29] play the primary role in maintaining the structure of the thread.

One possible explanation of the operating mechanism of the motor of the bacterial filament involves the fact that the torque is generated by a stream of protons between the

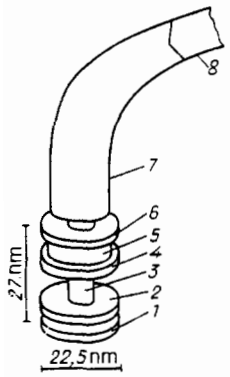

FIG. 5. Organization diagram of filament of *E. coli* and some other bacteria.[27] *1*–M-ring, *2*–S-ring, *3*–rod, *4*–P-ring, *5*–cylinder, *6*–L-ring, *7*–hamulus, *8*–filament thread.

M-ring of the basal body and the S-ring, attached to the rigid structure of the cell wall.[30,31] Glagolev and Skulachev suggested that such a transfer of protons is possible from an amino group located on the M-ring to a carboxyl acceptor group, located in the cytoplasmic membrane (Fig. 6). Calculations show that for one revolution of the motor a transfer of about 300 protons is necessary.[30]

It is interesting that the motors of individual flagella operate independently of each other.[54,55]

2.4. Change in behavior of individual bacterium in response to a change in external conditions

"A fish goes where it is deeper, and man—where it is better," this principle of the optimization of motion is usually satisfied not only by multicell organisms but also by bacteria. The behavior of bacteria is evident phenomenologically as a movement to a more favorable environment and away from less favorable.[99]

Berg, Koshland, and their colleagues have shown that the tumbling frequency (and, consequently, also the length of steady swimming) changes in an attractant or repellent gradient. If the bacteria happen to be swimming along an attractant gradient (i.e., in the "correct" direction), tumbling is partially suppressed and becomes more infrequent. In a repellent gradient the effect is the opposite.[14,56–58] By varying the tumbling frequency, bacterium undergoing a random walk is nevertheless gradually displaced in the direction of increase/decrease in the attactant/repellent concentration.

Oxygen, N-acetyl-D-glucosamine, D-galactose, D-glucose, L-aspartate, L-serine, and certain other compounds are attractants for colon bacillus (*E. coli*).[51,59–63] Fatty acids, alcohols, hydrophobic amino acids as well as many other substances are repellents.[51,63,64]

Not only chemical compounds but also physical factors can serve as attractants or repellents for bacteria: light,[51,65–70,83] temperature,[51,71–76] electric and magnetic fields,[51,77–79] and gravitation.[51,80–82] Thus, for example, high-intensity blue light initiates continuous tumbling of *E. coli* bacteria. It is assumed that this effect is due to the breakup of flavin molecules, which is accompanied by an oxidation of other hypothetical compounds controlling the behavior of bacteria.[47,65–67,83] One other example is the fact that varying electric fields can increase the mobility of *E. coli* bacteria, but at the same time they can inhibit (by about 70%) their chemotaxis capacity.[79]

It is significant that all the effects, associated with the action of attractants or repellents, occur not only in a spatial but also in a temporal gradient, i.e., as a result of a variation of concentration with time.[56,57] This means that bacteria have a memory.

2.5. Reception biophysics

In 1969 Adler established that bacteria sense attractants by means of a special set of tools called chemoreceptors.[59] The receptors are located in the cell membrane.[84] They are protein molecules, able to "measure" changes in the concentration of certain substances and to transmit the obtained information to the bacterial motor.[8,27,50,51,63,68,85]

The mechanism of bacterial chemoreception has not been precisely established. It is known that the receptor passes through the cell membrane. The outer part of the receptor (extending into the medium near the membrane, the periplasm) is able to bond to the aspartate molecule.[86,87] With this bonding the conformation of the receptor may be altered,[88–90] and as a result information as to whether the receptor is "occupied" enters within the cell into the cytoplasm.

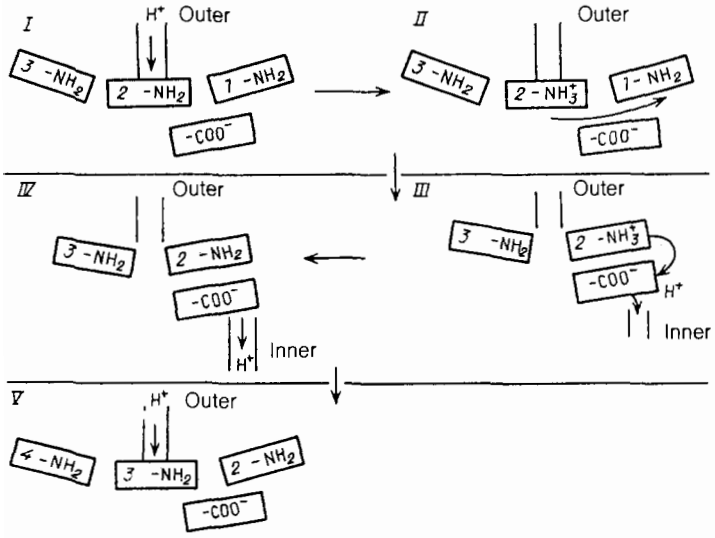

FIG. 6. Operating scheme of bacterial filament motor.[27] I–under the action of a proton-moving force a proton penetrates from the outer medium, charging the amino group of M-ring subunit; II–interaction of charged amino group with a carboxyl acceptor group leads to rotation of the M-ring; III–proton is transferred to acceptor and arrives inside cell; IV–mutual repulsion arises between carboxyl acceptor group and amino group, having a weak negative charge, which leads to a further rotation of the M-ring; V–site of subunit 2 of M-ring occupies subunit 3. It is assumed there are 15–17 proton channels per one basal body and a corresponding number of acceptor molecules.

TABLE II. Set of some *E. coli* and *D. typhimurium* receptors.

Most active chemoeffector for given receptor	Other substances which interact with the same receptor	Characteristic of: E. Coli	Characteristic of: S. typhimurium	Attractant (A) or repellent (R)
Glucitol		+		A
N-acetyl glucosamine		+		A
D-fructose		+		A
D-galactose	D-glucose, D-fucose	+	+	A
D-glucose		+		A
Aspartate	Glutamate	+	+	A
Serine	Cysteine, alanine, glycine	+	+	A
Acetate	Valerate, butyrate, propionate	+	+	R
Leucine	Isoleucine, valine	+	+	R
Phenol			+	R
Fumarate			+	A

Most receptors are highly specific with respect to one or two chemical compounds, but less specific receptors are also known. About fifteen receptors reacting to attractants are known, and about ten are known that react to repellents.[64,84,91-93] Each type of bacterium responds to its own set of attractants and repellents. For example, the *Salmonella typhimurium* bacteria are sensitive to phenol while *E. coli* are not.[94] A set of several *E. coli* and *S. typhimurium* receptors are given in Table II (taken from Ref. 84). The behavior of bacteria depends on the number of bound receptors.

It has been shown[95] that in an attractant gradient the time of steady swimming (in the interval between two tumblings) is given by the expression

$$T(u) = T_0(1 + b\gamma u), \tag{2}$$

where u is the cosine of the angle between the direction of motion and of the gradient, and γ is the reciprocal of the distance along the direction of the gradient over which the concentration of the attractant decreases by a factor of $1/e$. The constant b (in Eq. (2)) was measured experimentally and was found to be equal to 12 mm (for a serine concentration of 1 mM).[95] It is clear from Eq. (2) that the parameter b reflects the sensitivity of the chemotactic "set of tools" of bacteria to the attractant gradient.

The answer to the following question is of interest: does the absolute (dN/dt) or relative ($d\ln N/dt$) change in the number of bound receptors control the behavior of bacteria?

It has been shown[95] that one or the other answer to this question determines in a significant manner the character of the dependence of the sensitivity b (see Eq. (2)) of *E. coli* bacteria to a gradient of the attractant serine. This fact is reflected in Fig. 7. It is seen that in one case (b depends on $d\ln N/dt$) the sensitivity decreases monotonically with an increase in the concentration gradient, while in the other case (b depends on dN/dt) the sensitivity b reaches a maximum and then falls off. Experimental data (also shown in Fig. 7) indicate that the behavior of the bacteria is determined by the absolute change in the number of bound receptors.

Following the authors of Ref. 96, we will describe the receptor binding process by the function $p(t)$, which is equal to 1 when the receptor is bound and zero the rest of the time. The average value $\bar{p}$ depends on the dissociation constant K, i.e., on the value of the concentration of bound molecules (measured in moles per liter) for which $\bar{p} = 0.5$. Let us assume $C_{1/2}$ is this concentration, but measured as the number of molecules per cm^3. For the instantaneous concentration C

$$\bar{p} = C(C + C_{1/2})^{-1}. \tag{3}$$

A change in the number of bound receptors, produces a response–a change in the behavior of bacteria.[95] Thus, the response is proportional to $d\bar{p}/dt$, where $\bar{p}$ is determined by Eq. (3), and as a result, randomly walking bacteria are steadily displaced toward the higher attractant concentration. Such control is most effective if the measurements of the concentration C are made sufficiently rapidly: while the displacement of the bacterium is significantly less than the average length of steady swimming.[97] The time required for the chemotactic response in any case cannot exceed the interval τ_{rot}, which characterizes Brownian migration of the cell. Let us assume T is the time required by the cell to "measure" the value of $\bar{p}$, and $\bar{C}$ is the average concentration of the attractant to be bound by the cell receptors. The root-mean-square error of this measurement[96] is:

$$\Delta C_{rms}/\bar{C} = [2\pi TD\bar{C}NSa(1 - \bar{p})/(NS + \pi a)]^{-1/2}, \tag{4}$$

where a is the radius of the sphere within which the bacterium measures the attractant concentration, and N is the number of receptors on a bacterium. It is clear that two successive (within a time $2T$) measurements of the concentration $\bar{C}$ can cause a change in the bacterial behavior only if the difference in the measurement results exceeds the rms

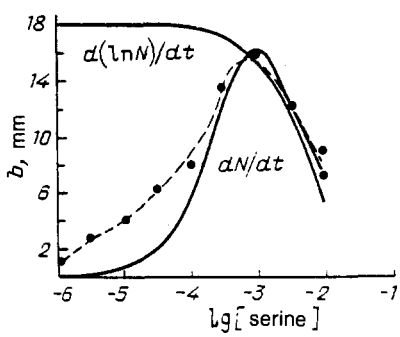

FIG. 7. Dependence of sensitivity to the gradient of the parameter b–from Eq. (2)–dependence on concentration of attractant (serine).[95] Theoretical curves (for the two models studied) are shown by solid lines and the experimental curve is the dashed line.

error, i.e.,

$$T/\bar{C}\cdot\partial\bar{C}/\partial t > \sqrt{2}\Delta C_{\rm rms}/\bar{C}. \quad (5)$$

As shown in Ref. 96, it follows from Eqs. (4) and (5) that

$$T > \left[\pi a D \frac{NS}{NS+\pi a}\frac{\bar{C}C_{1/2}}{\bar{C}+C_{1/2}}\left(\frac{1}{\bar{C}}\frac{d\bar{C}}{dt}\right)^2\right]^{-1/3} \quad (6)$$

Producing a temporal gradient of an attractant (L-glutamate) by means of enzymes, Brown and Berg[96] showed that the steady swimming time is doubled on the average (from 0.67 to 1.34 s) for $d\bar{p}/dt = 1.05\times10^{-3}\,s^{-1}$ ($\bar{C} = 1.61$ mM, $(1/\bar{C})\partial\bar{C}/\partial t = 4.35\times10^{-3}\,s^{-1}$, $C_{1/2} = 2.3$ mM). If $a = 0.8$ μm, $D = 9\times10^{-6}$ cm^2/s and[97] $NS/(NS+\pi a) = 0.5$, then $2T > 0.087$ s. The time interval necessary for detecting a time gradient equal to 1/10 of the value cited above must be, according to Eq. (6), $10^{2/3} = 4.64$ times longer which is about 0.4 sec.

Dahlquist and colleagues,[95] experimenting with the use of an artificially maintained spatial gradient of the attractant L-serine, showed that the length of steady swimming (about 10 μm) is doubled if the distance over which the gradient is maintained is about 1.4 cm. For $C_{1/2} = 1$ mM, $(1/\bar{C})\partial\bar{C}/\partial x = 0.7$ cm^{-1}, $V = 15$ μm/s, $a = 0.8$ μm, $D = 10^{-5}$ cm^2/s and[97] $NS/(NS+\pi a) = 0.5$, then $2T \geqslant 0.27$ sec. A gradient of 1/10 of the value cited above can be detected in ~ 1.2 s.

Mesibov and co-authors have published a paper,[98] where the threshold values are given for the attractants DL-α-methyl aspartate and D-galactose, stimulating a chemotactic response in *E. coli* bacteria. By using the data of this paper as well as some interpolations, obtained by Adler,[71] Berg and Purcell found[97] that for DL-α-methyl aspartate $2T > 0.6$ s while for D-galactose $2T > 1.4$ s.

All of the above-given estimates show that the time required for bacteria to detect a change in the concentration of an attractant is about 1 s. Longer times are forbidden by the effect of the random motion of the bacteria.[96,97] The chemotactic set of tools of bacteria takes this fact into account.

What is the mechanism of the short-term memory of bacteria? Macnab and Koshland suggested that there is some regulator (X) of the chemotactic response inside the cell.[57,84] A hypothetical scheme for the action of this (hypothetical) regulator is shown in Fig. 8. According to this scheme the X-regulator controls the tumbling frequency. In the absence of a spatial or temporal gradient of the attractant (or repellent) a constant average value of the quantity $X = X_{ss}$ is maintained inside the bacteria. If the instantaneous value of the quantity $X = X_{ss}$ fluctuates in accordance with a Poisson distribution about some critical value $X = X_{cr}$, then these fluctuations can govern the random walk of the bacteria in the absence of an attractant or repellent gradient in the external medium. For $X_{ss} > X_{cr}$ tumbling is suppressed. When $X_{ss} < X_{cr}$, tumbling becomes possible, and as a result the bacterium changes its direction of motion from time to time, executing a random walk.

Within the framework of this model it is easy to explain the reason for the change in behavior of bacteria in the presence of a change in the attractant or repellent concentration (Fig. 9). Namely, an increase in the attractant concentration causes an increase in the formation rate V_f of the regulator X, and in its dissociation rate V_d. However, as shown in Fig. 9a, V_f increases faster than V_d. As a result, the amount of the substance X in the cell increases temporarily. The action of a repellent is also explained in a similar manner (Fig. 9b). The return of the concentration of X to its original level makes it possible to explain the experimentally observed adaptation of the behavior of bacteria to an increased amount of attractant or repellent in the culture medium.[47,84,87,100–108] Thus, according to the model we have presented the quantity $(X_{ss} - X_{cr})$ controls the behavior of bacteria. Fluctuations of X_{ss} and/or X_{cr} (see Fig. 8) cause a transformation of steady swimming into tumbling and vice versa.

It is easy to calculate the probability that $X_{ss} > X_{cr}$ (or $X_{ss} < X_{cr}$). Let us assume the initial concentration of X is equal to X_{ss} ($X_{ss} = X_{cr}$). The probability density of a deviation of X from the value of X_{ss} will vary in time in accordance with the following law:

$$\rho(t) = \sum_{k=1}^{\infty} p_k g_k(t), \quad (7)$$

where p_k is the probability that random integral changes of this number, which starts from zero, will augment this number to a value equal (to be specific) to 1 after exactly k steps, while $g_k(t)$ is the probability density function of passing through k steps in a time t. By a step we mean a change of X_{ss} by unity. It can be shown[109,110] that

$$p_k = \frac{1}{k}\left[\frac{k}{(k+1)/2}\right]\cdot 2^{-k}, \quad (8)$$

and

$$g_k(t) = \frac{(2\lambda)^k t^{k-1} e^{-2\lambda t}}{\Gamma(k)}, \quad (9)$$

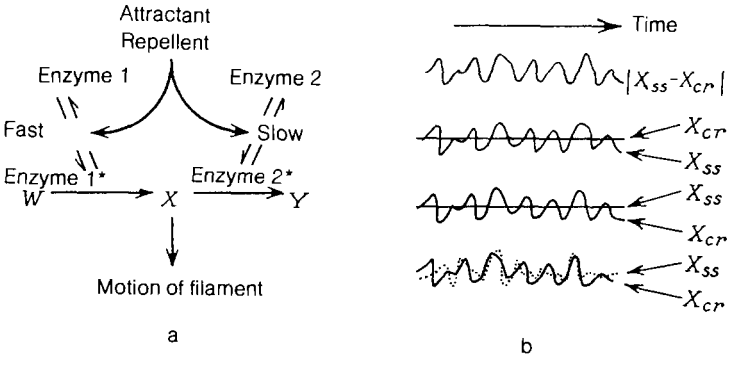

FIG. 8. Schematic representation of the action of regulator (X) of chemotactic response (Macnab–Koshland model).[57,84] a–Attractant alters conformation of enzymes 1 and 2, activating them. Enzyme 1 is activated rapidly while enzyme 2 is activated slowly. These enzymes (1 and 2), respectively, control the synthesis and decomposition of the substance X. The concentration of X increases with movement along the gradient, decreases with movement opposite to the gradient and remains constant when there is no gradient. b–Instantaneous value of the quantity $X = X_{ss}$ varies in a random manner with respect to some critical value X_{cr}. When $X_{ss} - X_{cr} < 0$ tumbling is produced. When $X_{ss} - X_{cr} > 0$, tumbling is suppressed. The value of $X_{ss} - X_{cr}$ can change as a result of fluctuations of X_{ss}, X_{cr} or of both of these quantities.

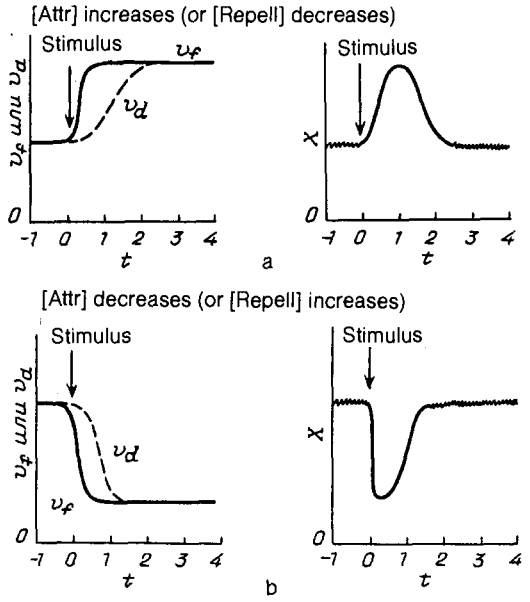

FIG. 9. Mechanism for a change in behavior of bacteria in response to a change in the attractant or repellent concentration (according to the Macnab–Koshland model).[84] a–Increase in concentration of attractant [Attr] (or decrease in concentration of repellent [Repell]) causes V_f to increase faster than V_d, which leads to a temporary increase in the concentration X and, as a consequence, to a decrease in the tumbling frequency. b–Decrease of concentration of attractant (or increase in concentration of repellent) causes V_f to decrease faster than V_d. This leads to a decrease in the concentration of X and a temporary increase in the tumbling frequency.

where $\lambda = k_f$ is the rate constant of the formation of the substance X (see Fig. 14), and $\Gamma(k)$ is the gamma function. Substitution of Eqs. (8) and (9) into (7) leads (after some manipulations) to the following relation:[110]

$$\rho(t) = \frac{e^{-2\lambda t} I_1(2\lambda t)}{t}, \tag{10}$$

where I_1 is the modified Bessel function of *I*st kind. The function (10) differs from an exponential. The case where $X_{ss} \neq X_{cr}$ also does not lead to an exponential behavior of $\rho(t)$.[110] However, the experimental data presented in Ref. 110 follow an exponential curve quite well. In particular, no prolonged intervals of clockwise (as well as counterclockwise) rotation of the flagella, as predicted by the Macnab–Koshland model described above, are observed in the experiment. For large t values the function (10) decreases with an increase in t as $t^{-3/2}$ and it cannot be reduced to exponential form.[110] Accordingly, Berg and his colleagues proposed a new model for regulating the transition from steady swimming to tumbling and vice versa:[110]

$$\text{Steady swimming} \underset{k_t}{\overset{k_r}{\rightleftharpoons}} \text{tumbling}. \tag{11}$$

This model is characterized by two states, between which the transition probability per unit time remains constant. Each of the states (steady swimming or tumbling) is characterized by the exponential dependence on the interval length and by the average lifetimes, equal to $1/k_r$ and $1/k_t$, respectively. The constants k_r and k_t in Eq. (11) give the probabilities (per unit time) of transition from steady swimming to tumbling and from tumbling to steady swimming. At the molecular level these constants can describe alternating conformations of certain protein. As experiments have shown, a chemotactic signal shifts k_r and k_t in opposite directions, but k_r changes more strongly than k_t.[110] In principle, the model (11) does not rule out the formation of an intermediate product X (as in the Macnab–Koshland model; see Fig. 8), but the rotation direction of the flagella in this situation cannot depend on the value of X_{cr} and, consequently, cannot depend on the fluctuations of the concentration X of the chemotactic response regulator.

It must be pointed out that the model (11) is apparently not valid for all types of bacteria. Experimental data exist indicating that the motion of halobacteria (in contrast to *E. coli* bacteria) can be determined by the quantity[223] X_{cr} and, consequently, can be described by the Macnab–Koshland model.

The variation (in a time[95] of ~ 1 sec) of the constants k_r and k_t in Eq. (11) adequately describes the behavior of the *E. coli* bacteria in response to a change in the concentration of attractants or repellents in the external medium. The change in the transition frequencies from steady swimming to tumbling and vice versa, specified by these constants, depends, as indicated above, on the rate of change of the number of receptors bound by attractant or repellent molecules, i.e., on the function dp/dt. This means that the bacteria must be able to compare the quantity p at the present instant of time to that in the recent past. In other words, the chemotactic response (i.e., the signal specifying the value of the constants k_r and k_t and denoted below by the letter R) is proportional to the difference $(p - A)$:

$$R = g(p - A), \tag{12}$$

where g is a constant of proportionality and A in the adaptation level; in turn, A varies in accordance with the equation[110,111]

$$dA/dt = \frac{p - A}{\tau}, \tag{13}$$

where τ is the adaptation constant. The value of the adaptation level A correlates with the methylation level (i.e., the binding of the CH_3 group of the intramembrane methyl-bonding chemotactic protein (the so-called MCP protein)). The adaptation process of a cell is related to the growth process of the methylation level, which in turn is triggered by the bonding of an attractant molecule (see, e.g., the review in Ref. 102). For $A = p$, according to Eq. (13), $dA/dt = 0$; i.e., the cell is completely adapted. The solution of Eq. (13) for $t \gg \tau$ is

$$A(t) = \frac{e^{-t/\tau}}{\tau} \int_0^t P(t') e^{t'/\tau} dt'. \tag{14}$$

It follows from Eqs. (12) and (14) that

$$R(t) = g\{p(t) - \frac{1}{\tau} \int_0^t p(t') \exp[(t'/\tau) - t] dt'\}. \tag{15}$$

The first term inside the curly brackets in (15), $p(t)$, characterizes the number of receptors bound at a given instant. The second term in (15) is the average of the function p over all past time with a weighting factor, which decreases exponentially with time. This weighting factor is what describes the memory of the bacteria. According to Eq. (15), information

about the number of bound receptors is retained only over times not much greater than the adaptation constant τ.

Thus, the memory of bacteria is attributable to the adaptation of cells to the ambient medium; this adaptation is based on the methylation processes of intramembrane MCP proteins. The memory makes it possible for bacteria, using the receptors, to compare the concentrations of attractants or repellents at points located along the trajectories of the bacteria. The information obtained by this comparison is used to adjust the tumbling frequency.

2.6. Bacteria as individuals

In 1947 Luria and Latarjet[112] discovered that it is impossible to annihilate completely a population of bacteria by high doses of ultraviolet or x-radiation. From 10^{-2} to 10^{-4} of the total number of cells survive. This does not rule out the possibility that the surviving cells owe their resistance to the fact that they are in a state of severely retarded growth. The mechanism for this retardation is not clear up to this point.[113] It is clear, however, that the physiological state of the surviving cells is different from the physiological state of most of the cells of the population. In other words, bacterial populations are heterogeneous in a certain sense. The cells comprising these populations, it turns out, are endowed with individual properties. These properties appear not only in a differentiated survival of bacteria, but also in the difference in their behavior in the same culture medium.[114] The behavior of cells was investigated in Ref. 114 by means of the attachment of cell flagella to glass by means of an antibody, and then the rotation direction of the cells was recorded (on video tape). The experiments were based on the fact that counterclockwise and clockwise rotation of the attached cells (viewed along the axis passing through the attached flagellum) are equivalent, respectively, to tumbling or steady swimming of freely floating bacteria.[48] It was found that individual bacteria (*S. typhimurium*) are characterized by their own specific time intervals of steady swimming both in response to α-methyl aspartate (causing prolonged clockwise rotation) and also in its absence. For different bacteria these intervals can differ by a factor of two. Moreover, it was established that the clockwise rotation time (equivalent to the steady swimming time of a free cell) in the absence of α-methyl aspartate correlates linearly with the duration of the steady swimming intervals in response to the presence of α-methyl aspartate (which is an attractant) (Fig. 10); no such correlation exists for the counterclockwise rotation time, which corresponds to tumbling.[114] An impression is created that the individuality in the behavior of bacteria is caused by the chemotactic responses of the micro-organisms to attractants but not to repellents.[51] Spudich and Koshland[114] explained individual differences by a small number of molecules regulating the rotation direction of the filament. Variations of this small number of molecules, caused by random factors in the course of individual development, can cause differences between cells. Within the framework of the model (11) this means that each cell has its own individual set of values of the constants k_r and k_l.

It is obvious that the greater the diversity of the members of a population, the higher the probability for survival under extreme conditions and the greater adaptation capabilities of the bacteria.

2.7. Chemotaxis and evolution

Chemotaxis apparently arises in the very early stages of development.[101,115] Known experimental data indicate that chemotaxis of bacteria and chemotaxis of specialized eucaryotic cells (from which multicell organisms are formed) have much in common. It is certainly possible, for example, that the hormonal systems of animals and man were developed in earlier existing systems, providing for the chemotactic functions of single-cell organisms.[101] Therefore, studies of chemotaxis (in particular, its role in pattern formation processes) can bring us closer to an understanding of the general laws governing the development of living systems.

3. PATTERN FORMATION IN BACTERIA POPULATIONS

3.1. Population waves as a cooperative chemotactic response of bacteria

In the middle and late 1960s Adler and his co-workers established that bacteria, locally inoculated into a culture medium, can form propagating population waves (Fig. 11).[59,118-121] It was shown that these waves are macroscopic phenomena, produced by microeffects, namely, by a change in the tumbling frequency of each of the bacteria in the presence of a change in the concentration of some attractant. The local decrease in the concentration of an attractant is caused by its consumption by the bacteria, and thus a gradient of

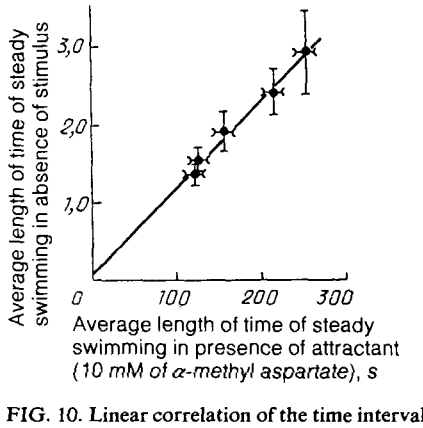

FIG. 10. Linear correlation of the time intervals of steady swimming of a free cell in the absence and in the presence of an attractant.[114]

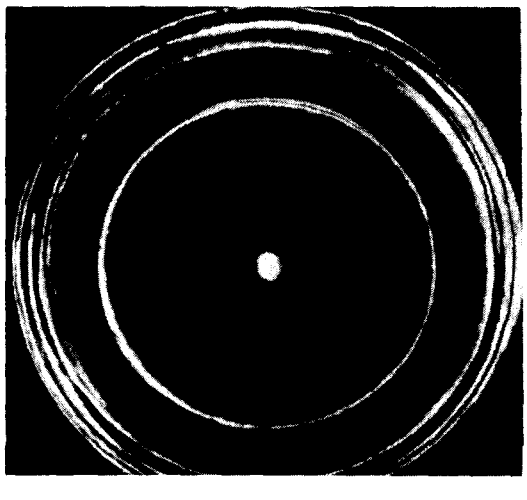

FIG. 11. Concentric bacterial population wave in Petrie dish.[116]

this concentration arises. Within the chaotic motion of the bacteria a component appears that is directed along the gradient. Moreover, the bacteria continue to multiply. As a result, a population wave is formed that is easily discernible by the naked eye. This wave actually renders visible the boundary between a region of reduced attractant concentration (as an example, within the expanding annular front in Fig. 11) and the region where the attractant concentration is still high.[59,116,118-121]

A mathematical model of the motion of this wave was suggested by Keller and Segel[122,123] in 1971. Let us assume $f(c)$ is the mean tumbling frequency during motion in a given direction, and c is the mean concentration of the attractant (or substrate) consumable by the bacteria, and is a function of the coordinate x. We will define the function $n(x)$ as the density of cells at the point x. The flux of bacteria $J(x)$ per unit time in the direction of increasing x is[122]

$$J(x) = \int_{x-\Delta}^{x} f[c(s + \frac{1}{2}\alpha\Delta)\ \text{ln}s]ds - \int_{x}^{x-\Delta} f[c(s - \frac{1}{2}\alpha\Delta)\ \text{ln}s]ds. \quad (16)$$

Using the approximation that is often employed in theoretical studies of Brownian motion,[124] we write Eq. (16) in the following form:

$$J(x) = \Delta^2[-f(c(x))\mathrm{d}n(x)/\mathrm{d}x + (\alpha - 1)\mathrm{d}f/\mathrm{d}c \cdot n(x)\mathrm{d}c/\mathrm{d}x],$$

or

$$J(x) = -\mu \mathrm{d}n/\mathrm{d}x + \chi n \mathrm{d}c/\mathrm{d}x. \quad (17)$$

In Eq. (17) the mobility is

$$\mu(c) \equiv \Delta^2/\Delta t = f(c)\Delta^2,$$

where $\Delta t \equiv 1/f(c)$ is the mean time interval between two successive tumblings, and the chemotactic coefficient is

$$\chi(c) = (\alpha - 1)\Delta^2 \mathrm{d}f/\mathrm{d}c,$$

so that

$$\chi(c) = (\alpha - 1)\mathrm{d}\mu/\mathrm{d}c.$$

Since

$$\partial n/\partial t = -\nabla J,$$

where[125]

$$J = -\mu \nabla n + \chi n \nabla c,$$

then (for the one-dimensional case)

$$\frac{\partial n}{\partial t} = -\frac{\partial}{\partial x}(-\mu \frac{\partial n}{\partial x} + \chi n \frac{\partial c}{\partial x}). \quad (18)$$

The first term on the right side of (18) is the motion of the bacteria in the absence of chemotaxis, while the second term describes the chemotactic response of the bacteria.

The concentration of the culture substrate (which is an attractant for bacteria) also changes (according to the Keller–Segel model[123]) in accordance with the equation

$$\frac{\partial c}{\partial t} = -k(c)n + D\frac{\partial^2 c}{\partial x^2}, \quad (19)$$

where $k(c)$ is the consumption rate of the substrate by a cell, and D is the diffusion constant of the substrate. It is assumed that the substrate concentration is quite high and does not limit its consumption rate, i.e., k is a constant in the Keller–Segel model.[123]

The solution of the system of differential equations (18) and (19) can be obtained in analytical form with certain additional assumptions. Let us take

$$D = 0. \quad (20)$$

Then, using the substitution

$$n(x, t) = n(\xi), \quad c(x, t) = c(\xi), \quad \xi = x - at, \quad (21)$$

we obtain

$$ac' = kn, \quad (22)$$

$$an' = (\chi n c')' - \mu n''. \quad (23)$$

In the system of Eqs. (22) and (23) the differentiation is with respect to the variable χ. The system of Eqs. (22) and (23) was solved in Ref. 117 for the following obvious boundary conditions:

$$n \to 0, \quad n' \to 0, \quad c \to c_\infty \quad \text{as} \quad \xi \to \infty. \quad (24)$$

Integrating (23), we obtain

$$an = \chi n c' - \mu n' + \text{const}. \quad (25)$$

With the boundary conditions (24) taken into consideration the constant is equal to zero. The integration of Eq. (25) yields

$$n = Qe^{g(c)/\mu}e^{-\bar{\xi}}, \quad (26)$$

where $g' \equiv \chi$, $\bar{\xi} = (a/\mu)\xi$. It is easy to obtain

$$\mathrm{d}c/\mathrm{d}\xi = Qka^{-1}e^{g(c)/\mu}e^{-\bar{\xi}}. \quad (27)$$

from Eqs. (22) and (26). Since c increases monotonically, we can consider ξ as a function of c. Then it follows from Eq. (27) that

$$\xi = \ln\{Qk\mu a^{-2}[\int_{c}^{c_\infty} e^{-g(p)/\mu}\mathrm{d}p]^{-1}\}. \quad (28)$$

As shown in Ref. 123, the solution of Eq. (28) exists for

$$\chi(c) = \delta c^\alpha, \quad (29)$$

where δ is a constant and $\alpha \leqslant -1$.

By integrating Eq. (22) with Eqs. (26) and (29) taken into account, we obtain[123]

$$c = [Qka^{-2}(\delta - \mu)e^{-\bar{\xi}} + c_\infty^{1-\bar{\delta}}]^{-1/(\bar{\delta}-1)}. \quad (30)$$

In Eq. (30) $\bar{\delta} = \delta/\mu$, $\alpha = -1$. If we assume[123] that

$$Qka^{-2}(\delta - \mu) = c_\infty^{1-\bar{\delta}}, \quad (31)$$

Eq. (30) can be rewritten in the following form:

$$\frac{c}{c_\infty} = (1 + e^{-\bar{\xi}})^{-1/(\bar{\delta}-1)}. \quad (32)$$

The corresponding expression for n becomes

$$\frac{n}{a^2 c_\infty (\mu k)^{-1}} = \frac{1}{\bar{\delta} - 1} e^{-\bar{\xi}}(1 + e^{-\bar{\xi}})^{-\bar{\delta}/(\bar{\delta}-1)}. \quad (33)$$

As $\bar{\xi} \to -\infty$, Eqs. (32) and (33) will have finite solutions if

$$\bar{\delta} > 1, \quad \text{or} \quad \delta > \mu.$$

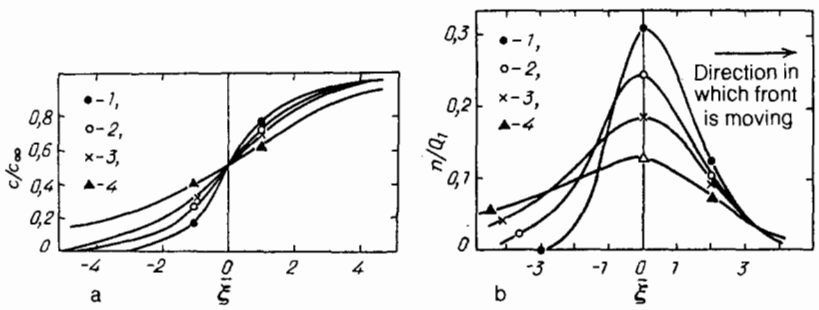

FIG. 12. Dependence of the quantities c/c_∞ (a) and n/Q_1 (b), where $Q_1 = a^2 c_\infty/\mu k$, on $\bar{\xi}$ (in units of μ/a; a is the velocity of the population wave) for $\delta/\mu = 4/3$ (curve *1*), 2 (*2*), 3 (*3*), and 5 (*4*).[123] It is seen that the weaker the chemotactic response, the narrower the population wave.

Then

$$\lim_{\bar{\xi}\to-\infty} c = 0, \quad \lim_{\bar{\xi}\to-\infty} n = 0. \tag{34}$$

The curves described by Eqs. (32) and (33) are shown in Fig. 12.

Since these solutions are obtained with the assumption (20), it is interesting to evaluate to what extent this assumption agrees with reality. For this purpose let us find the ratio of the two terms on the right side of Eq. (19) with the substitution (21) taken into account: $(Dd^2c/d\bar{\xi}^2)/kn$. As $\bar{\xi}$ varies from $-\infty$ to ∞, this ratio varies from $(D/\mu)\bar{\delta}/(\bar{\delta}-1)$ to D/μ.[123] It follows from this that condition (20) reflects reality if the diffusion constant D is small compared with μ. The most actively diffusing attractant is oxygen, for which[126] $D \sim 5\times 10^{-2}$ cm^2/h. This value is smaller than the value $\mu = 0.25$ cm^2/h, obtained in Ref. 120. In this situation the approximation (20) can obviously be used. However, according to other estimates[127] $\mu \sim 5\times 10^{-3}$ cm^2/h. In this case $D/\mu = 10$, so that the use of the approximation (20) is unjustified and the system of Eqs. (19)–(20) must be solved by numerical methods.

The Keller–Segel model is a phenomenological one. This means that there is no clear physical interpretation of the functions μ and χ (Eq. (18)), and there is also a gap between models for the behavior of individual bacteria and for communities of bacteria.

In principle, one could attempt to describe the motion of a cell population, starting from a detailed analysis of the motion of the individual cells. Such an investigation procedure—from microscopic events to macroscopic effects—would possibly allow one to ascribe real physical meaning to the functions and parameters describing the behavior of cell populations (as an example, the chemotactically caused motion of a bacterial wave). Some of the experimental data necessary to implement such a program have already been gathered. For example, Berg and Brown[14] carried out an investigation of the motion of *E. coli* bacteria in response to a chemotactic stimulus: the motion of individual leucocytes,[128–131] slime ameba,[132–136,157] muscle fibroblasts,[137] and myxoplasms[138] was also investigated.

Piecewise-smooth curves, interrupted by abrupt changes in the direction of motion (as in Fig. 2), are a good approximation of the paths of motion of all of these cells. Let us determine how these parameters, characterizing the random walk of a single bacterium, are related to the parameters that determine the motion of population waves, μ and $V_d = \chi\nabla C$ in the system of Eqs. (18) and (19). The parameters μ and V_d can be related to the mean distances traversed by the cells during a time t by the following formulas:[124]

$$\mu \sim \lim_{t\to\infty}\left[\frac{1}{t}(\langle r_t^2\rangle - \langle r_t\rangle\langle r_t\rangle)\right], \tag{35}$$

$$V_d \sim \lim_{t\to\infty}\left[\frac{1}{t}\langle r_t\rangle\right]. \tag{36}$$

If there is no drift due to the action of external factors, then $\langle r_t\rangle = 0$ and, according to Eqs. (35) and (36),

$$V_d = 0, \quad \mu \sim \lim_{t\to\infty}\left[\frac{1}{t}\langle r_t^2\rangle\right].$$

During the time t the bacterium travels in the x direction (for example, along an attractant gradient) a distance

$$x_t = \sum_{c=i}^{n}\int_0^{\tau_i} x_i(s)\,ds, \tag{37}$$

where

$$t = \sum_{i=1}^{n}\tau_i.$$

Let us take $\phi_i(s)$ as the angle between the instantaneous velocity $\mathbf{V}(s)$ of the bacterium and the vector $\mathbf{x}$. Then

$$\langle x_t\rangle = \langle\sum_{i=1}^{n}\int_0^{\tau_i} V_i(s)\cos\phi_i(s)\,ds\rangle. \tag{38}$$

If the velocity does not change between tumblings, then Eq. (38) can be rewritten in the following form:

$$\langle x_t\rangle = \langle\sum_i V_i\tau_i\cos\phi_i\rangle$$

or[141]

$$\langle x_t\rangle = \sum_{i=1}^{n}\int V_i\tau_i\cos\phi_i P(\{V_i\};\{\tau_i\};\{\phi_i\})\,d\{V_i\}\,d\{\tau_i\}\,d\{\phi_i\}. \tag{39}$$

In Eq. (39) P is the probability that the bacterium is moving along the ith portion of the path with the velocity V_i during the time τ_i, and the ith portion is oriented at the angle ϕ_i with respect to the x axis. The function P can be specified if we make the following assumptions: 1) the random walk of the cells is a Markovian process; 2) the velocity does not depend on the direction; 3) the distribution of the path segments between two successive tumblings is exponential; 4) the random walk process of the cells is in a steady state and 5) this process is spatially isotropic. Then[141]

$$\langle x_t\rangle = \frac{1}{2\pi}\,n\int_0^\infty P(V)V\,dV\int_{-\pi}^{\pi}\cos\phi\,d\phi\int_0^\infty \tau\lambda(\phi,V)e^{-\lambda(\phi,V)\tau}\,d\tau, \tag{40}$$

where λ is the frequency of the tumblings. In accordance with available experimental data[95,97] the mean value of λ is

proportional to the rate of change dN/dt of the relative number of receptors bound by a chemoattractant (see also Fig. 7). This has provided a basis for assuming[141] that

$$\langle \ln \lambda \rangle = \begin{cases} \ln \lambda_0 - \alpha dN/dt, & \text{if } dN/dt > 0, \\ \ln \lambda_0 \text{ otherwise.} \end{cases} \quad (41)$$

In Eq. (41) (see Ref. 98)

$$\frac{dN}{dt} = \frac{K}{(K+c)^2}\frac{dc}{dt}, \quad (42)$$

where K is the dissociation constant for the complex of attractant with receptor. If $dc/dt = V\cos\phi\, dc/dx$, then it follows from Eqs. (41) and (42) that

$$\langle \lambda \rangle^{-1} = \begin{cases} \lambda_0^{-1} + \varepsilon V\cos\phi, & \text{if } |\phi| < \pi/2, \\ \lambda_0^{-1}, & \text{if } |\phi| \geq \pi/2, \end{cases} \quad (43)$$

where

$$\varepsilon \equiv \frac{\alpha K c}{\lambda_0 (K+c)^2}\frac{d\ln c}{dx}. \quad (44)$$

Then from Eqs. (39) and (43) one can derive the following expression:[141]

$$\langle x_t \rangle = \frac{\varepsilon}{4} n \langle V^2 \rangle, \quad (45)$$

where

$$\langle V^2 \rangle = \int_0^\infty V^2 P(V)\, dV,$$

and ε is defined by the formula (44).

With formulas (36) and (43) taken into consideration it can be shown[141] that

$$t = n\lambda_0^{-1} + o(\varepsilon), \quad (46)$$

if ε, as well as the total tumbling time τ_w are small quantities. Finally, it follows directly from (36), (44) and (45) that

$$V_d \approx \frac{\alpha}{4}\langle V^2 \rangle \frac{Kc}{(K+c)^2}\frac{d\ln c}{dx}. \quad (47)$$

If the time τ_w is not small, then the value of V_d will be determined by the following expression[141] instead of Eq. (47):

$$V_d \approx \frac{\alpha\langle V^2 \rangle}{4(1+\lambda_0\tau)}\frac{Kc}{(K+c)^2}\frac{d\ln c}{dx}. \quad (48)$$

The parameter μ, defined by Eq. (35), can also be related to the parameters characterizing the random walk of a cell (see Refs. 132 and 139–142):

$$\mu \sim \lambda_0^{-1}(\langle V^2 \rangle - \langle V \rangle^2 + \frac{\langle V \rangle^2}{1 - \langle \cos\phi \rangle}). \quad (49)$$

Formulas (47)–(49) relate the macroscopic quantities μ and $V_d = \chi\nabla c$ of Eq. (18) to the microscopic parameters V, K, c, λ_0, τ_w. It is assumed here, of course, that the phenomenological Eqs. (18) and (19) are correct. However, how justified is this assumption?

In order to approach this question, one can attempt to derive Eqs. (18) and (19) from more fundamental kinetic equations. Such an attempt was made by Zaval'skiĭ and his colleagues.[143–145]

According to their model, chemotaxis is described by an equation of the form[144]

$$\frac{df(\mathbf{r}, \mathbf{n}, t)}{dt} + V\mathbf{n}\nabla f(\mathbf{r}, \mathbf{n}, t) = -\gamma(V, \mathbf{n}, \partial c/\partial t, \nabla c) f(\mathbf{r}, \mathbf{n}, t)$$

$$+ \frac{1}{4\pi}\int_{\mathbf{n}} \gamma(V, \mathbf{n}, c, \partial c/\partial t, \nabla c)\beta(\mathbf{n}, \mathbf{n}') f(\mathbf{r}, \mathbf{n}', t)\, d\mathbf{n}', \quad (50)$$

where f is the distribution density of the cells moving in the direction $\mathbf{n}$ in the vicinity of the point $\mathbf{r}$ at time t; γ is the tumbling frequency, $\beta(\mathbf{n}, \mathbf{n}')$ is the probability that a bacterium, moving in the $\mathbf{n}$ direction before tumbling, will be moving in the $\mathbf{n}'$ direction after it. Following Zaval'skiĭ,[145] we will assume that the interaction of receptors with the substrate is described by the first-order equation (42), where

$$\frac{dc}{dt} = \frac{\partial c}{\partial t} + V\nu\frac{\partial c}{\partial x}. \quad (51)$$

In Eq. (51) $V = \text{const}$ is the velocity of motion of the bacterium in a medium with a constant gradient of the chemoeffector concentration, with the direction of the gradient making an angle with the x axis whose cosine is equal to ν, and $\partial c/\partial t$ is defined by Eq. (19). Substituting the formulation (51) of the function dc/dt into Eq. (42), we obtain:

$$\frac{dN^*}{dt} = \frac{KN_0}{(K+c)^2} V\nu\frac{\partial c}{\partial x}, \quad (52)$$

where N^* is the absolute number of bound receptors and N_0 is the total number of receptors for a given chemoeffector. The derivation of (52) took into account that according to available experimental data[145] $\partial c/\partial t \ll V\nu\partial c/\partial x$. The changeover from Eq. (42) to (52) actually means a transition from "temporal" reception to "spatial" reception.

According to the experimental data of Brown and Berg,[96] the function γ from Eq. (50) has the following form:

$$\gamma = \gamma_0 \exp(-\alpha dN^*/dt), \quad (53)$$

where α is a proportionality coefficient depending on the strain of bacteria and the type of receptor. With Eq. (52) taken into consideration, formula (53) can be rewritten in the following form:

$$\gamma = \gamma_0 \exp(-\Psi\nu), \quad (54)$$

where

$$\Phi = \frac{\alpha N_0 K}{(K+c)^2} V\frac{\partial c}{\partial x}. \quad (55)$$

In principle, the microscopic parameters entering into Eq. (55) can be determined experimentally.

In order to plot the function $\beta(\mathbf{n}, \mathbf{n}')$ from Eq. (50) Zaval'skiĭ[145] used the results of the experiments of Berg and Brown;[14] he approximated the function β by a third-degree polynomial:

$$\beta(\mathbf{n},\mathbf{n}') = 3\pi(1 + 4\langle \mathbf{n},\mathbf{n}' \rangle - \langle \mathbf{n},\mathbf{n}' \rangle^2 - 4\langle \mathbf{n},\mathbf{n}' \rangle^3), \quad (56)$$

where we denote the cosine of the angle between the vectors $\mathbf{n}$ and $\mathbf{n}'$ by $\langle \mathbf{n}, \mathbf{n}' \rangle$.

After substitution of the functions (54) and (56) into Eq. (50) one can obtain in the diffusion approximation[145]

$$\frac{\partial n}{\partial t} - \frac{V}{3}\frac{\partial}{\partial x}[\frac{1}{\omega_1^1}(V\frac{\partial n}{\partial x} + \omega_0^1 n)] = 0, \quad (57)$$

where

$$\omega_0^1 = -\frac{1}{5}(\Psi + \frac{1}{10}\Psi^3 + \frac{1}{280}\Psi^5 + \frac{1}{15\,120}\Psi^7 + \ldots), \quad (58)$$

$$\omega_1^1 = \frac{1}{5}(1 + \frac{1}{6}\Psi^2 + \frac{1}{120}\Psi^4 + \frac{1}{5040}\Psi^6 + \ldots) + \frac{2}{75}(\Psi^2 + \frac{1}{14}\Psi^4 + \frac{1}{504}\Psi^6 + \ldots), \quad (59)$$

and n is the density of bacteria. It is interesting that Eq. (57) with the coefficients (58) and (59) was obtained without any limitations on the value of the substrate–chemoeffector concentration gradients (according to Eq. (55) these gradients determine the function ψ in Eqs. (58) and (59)). In particular, if the function $\partial c/\partial x$ is so small that $\psi \ll 1$, one can ignore second-order terms in the expansions (58) and (59) and then (57) can be reduced to the following form:[145]

$$\frac{\partial n}{\partial t} - \frac{5V^2}{3\gamma_0}\frac{\partial n^2}{\partial x^2} + \frac{V}{3}\Psi\frac{\partial n}{\partial x} + \frac{V}{3}\frac{\partial \Psi}{\partial x}n = 0. \quad (60)$$

Equation (60) is identical in form to the phenomenological equation (18), but unlike (18), all functional parameters in (60) have a clearly defined physical meaning. However, an analysis of the experimental data of Adler,[118,119] conducted by Zaval'skiĭ,[145] showed that $\psi \geqslant 1$ usually. Therefore, the transition from Eq. (57) to (60) may turn out to be invalid. This means that the coefficients μ and χ used in Eq. (18) cannot be expressed by means of simple analytical functions. Estimates carried out in Ref. 145 showed that the coefficient μ used to estimate the mobility of bacteria (for example, from formula (49)) can in fact greatly exceed the mobility values observed experimentally. This fact may explain the large differences between the estimates of μ, obtained in Refs. 120 and 127 (it must be pointed out that the parameter μ can be estimated theoretically only with difficulty[146]). Thus, the kinetic Eq. (50) evidently models the cooperative chemotactic response of bacteria (appearing in the form of a propagation of population waves) more adequately than the phenomenological formula (18).

The results of experimental and theoretical investigations presented above clearly demonstrate that chemotaxis can lead to the appearance of strong spatial nonuniformities in living systems (for example, in cell populations).

It is interesting, however, that chemotaxis of cells is not a necessary condition for the appearance of population waves. In the absence of chemotaxis such waves can arise as the result of the dependence of the mobility of the bacteria on the concentration of the substrate (for example, in the following form:

$$\frac{\mu(c)}{\mu_0} = 1 + \frac{4cc_0}{(c + c_0)^2},$$

where μ_0 and c_0 are constants[228]) or as the result of balanced growth and death of moving individuals in a random manner.[229,230]

Another interesting example of the collective behavior of bacteria, giving rise to a patterning of their populations, is the phenomenon of swarming.

3.2. Swarming of bacteria

This phenomenon was found for bacteria of the *Proteus* genus[147] and it appeared as a special type of motion of bacteria called swarmers, exceeding (in the swarming state) usual bacteria by a factor of tens in length and by a factor of hundreds in the number of filaments.[149] Swarmers perform a collective radial movement (swarming) and after a certain time, equal to the swarming period[150] ($\sim$1–3 hours), they provide the origin for a new colony of normally dividing cells, characterized by a normal length and number of filaments. Then the swarming is resumed. As a result, the surface of the culture medium is covered by annular populations, concentric about the point of inoculation (Fig. 13).

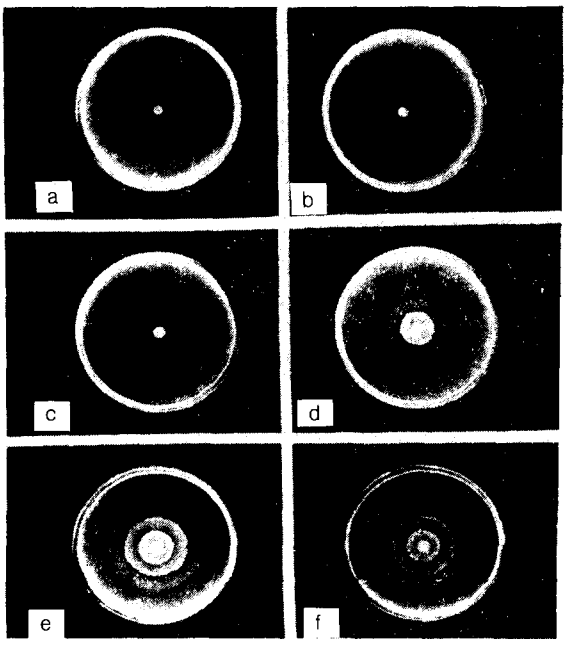

FIG. 13. Swarming of *Proteus mirabilis* bacteria, after 2 h (a), 3 h (b) 4 h (c), 8 h (d), 12 h (e) and 16 h (f) from time of inoculation.[150]

Several hypotheses have been suggested concerning the mechanisms for the swarming of bacteria. The most widespread is hypothesis of negative chemotaxis,[151] according to which the *Proteus* bacteria during their vital activity give off toxic metabolism products, inhibiting cell division. According to the hypothesis this also causes the unusually large length of the swarmers. The diffusion of the toxic agents through agarized culture medium in which the cell population is growing can cause in this case the formation of a gradient of these toxic agents. Negative taxis initiates a motion of the swarmers opposite to the gradient, which continues until the concentration of the cell metabolism products falls below some threshold value. The cell division and growth are then resumed, which causes in turn an increase in the concentration of the toxic agents given off by the cells. As a result, the swarming process is repeated after a certain time.

The "theory of positive taxis"[152] is no different in principle from the "hypothesis of negative taxis".[151] According to the former theory, the concentration of the nutrient decreases in the growth region of the bacterial population, leading to the formation of a gradient in this concentration. Swarmers appear as a result of a lack of nutrients. Their chemotactic response to an increase in concentration of the culture substrate with distance from the growth zone results in a directed motion, i.e., a swarming of bacteria. Then the process is repeated.

Experimental results, however, have not confirmed ei-

ther of these hypotheses.[151] It was found that swarming of bacteria is not related to chemotaxis.[153] As a consequence of this discovery, a new mechanism for this phenomenon was suggested to expain the swarming of bacteria: namely, "a genetic trigger", operating in a self-oscillatory regime.[154] The swarming mechanism proposed in Ref. 154 relates the synthesis of the protein flagelline, which comprises the filaments, to the synthesis of some hypothetical protein P_3, necessary to complete the bacteria division processes. The hypothetical scheme for the operation of the trigger is as follows: the volatile product P_2 of the bacterial metabolism removes the catabolitic repression with the synthesis of flagelline P_1, and during the subsequent competition over the common substrate S (intracellular amino acid pool) the synthesis of P_3 falls off sharply. Switching of the trigger to the normal synthesis of P_3 (the second stable state) is not attributable to external conditions, but is determined by the intracellular processes themselves, i.e., the swarming period is an intrinsic characteristic of the trigger. This picture does not contradict existing experimental data.[154,155] The motion of the swarmers is a consequence of their ability to move over the surface of a solid medium coated with a liquid film. Chemotaxis cannot be the cause of this motion because the metabolism product P_2 is assumed to be volatile. A simple mathematical model of swarming was proposed in Ref. 154:

$$\frac{\partial P_1}{\partial t} = f_1(P_1, P_2, S) + \nabla(D(P_1)\nabla P_1), \quad D \sim P_1^n (n > 1),$$

$$\frac{\partial P_2}{\partial t} = f_2(P_1, P_2, S), \tag{61}$$

$$\frac{\partial S}{\partial t} = f_3(P_1, P_2, S).$$

Within the framework of the model (61) the motion of the cluster of swarmers can be considered as the motion of flagelline P_1 with a diffusion constant $D(P_1)$. The $D \sim P_1^n$ dependence reflects both the collective character of the swarming as well as the finite propagation speed of the swarmers.[148] The observed pattern of *Proteus* populations (see Fig. 13) can be interpreted in terms of the theory of autowave processes[10,156–167] as the result of the motion of the flagelline front, whose amplitude and propagation velocity undergo relaxation oscillations in time. Unfortunately, it is not possible to specify the form of the functions f_1, f_2 and f_3 in the Eqs. (61) in view of a lack of experimental data. Thus, it is impossible, in particular, to exclude *a priori* the possibility of a relationship between swarming and the functional interdependence of the motion of bacteria and their growth.[168,169]

3.3. Aggregation of myxomycetes

The cooperative behavior of microorganisms has been investigated in greatest detail for the *Dictyostelium discoideum* myxomycetes.[132–136,157] The life cycle of this slime is shown in Fig. 14. It is seen from Fig. 14 that *Dictyostelium discoideum* can exist both in the form of individual amebas (stage 1) and also in the form of a multicell organism (stage 6). Stage 1 is accompanied by active cell divisions and it continues as long as the culture medium is rich in nutrients. The collective form of the amebas sets in with depletion of the nutrients. In this situation the individual cells become

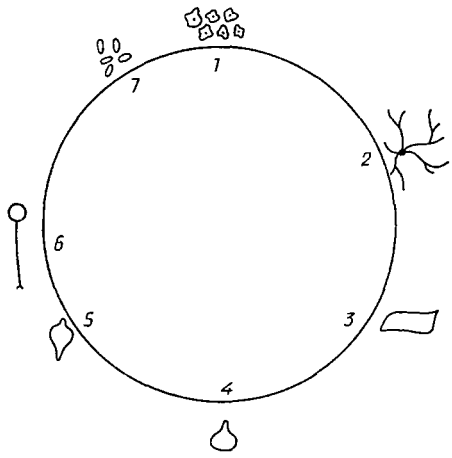

FIG. 14. Schematic representation of life cycle of the *Dictyostellium discoideum* slime.[136] *1*–free-living ameba, *2*–aggregation, *3*–migrating slime, *4*–early culmination, *5*–developed culmination, *6*–formation of fertile body, filled with spores, *7*–spores.

centers of aggregation, collecting from the surrounding territory (an area of ~ 1 cm^2) about 10^5 cells at each such center.[133,170] The aggregation occurs as a result of the chemotaxis of the individual amebas to an attractant, periodically released by the aggregation centers, namely, to cyclic adenosine monophosphoric acid (cAMP). If the concentration difference of the cAMP at opposite sides of a cell exceeds some threshold value ($\sim 10^{-12}$ M), the cell begins to move in the direction of increasing concentration.[133] The distribution of the cAMP in the medium is established by the action of the following processes: 1) synthesis in the cells; 2) diffusion through the volume; 3) decomposition (due to the action of a special enzyme).[133,157]

A mathematical model, describing the aggregation process of myxomycetes, was proposed in Ref. 134. This model in many respects is similar to the Keller–Segel model described above.[122,123,125] It is a system of two differential equations:

$$\frac{\partial a}{\partial t} = \nabla(D_a \nabla a - D_c \nabla \rho),$$

$$\frac{\partial \rho}{\partial t} = \nabla(D_\rho \nabla \rho) + f(\rho, a) - k(\rho, a), \tag{62}$$

where $a = a(\mathbf{r}, t)$ and $\rho = \rho(\mathbf{r}, t)$ are the concentrations of the amebas and cAMP molecules, respectively, D_a and D_ρ are their diffusion constants, and the coefficient D_c characterizes the strength of the chemotactic response of the individual cells; f is the synthesis rate of cAMP and k is its decomposition rate. A judicious choice of the functions f and k is a separate problem[134] and, of course, the available experimental data[133,135,136] must be taken into consideration. An analysis of the model (62) showed that the chemotaxis effect makes it possible to describe quite completely the aggregation process of individual amebas (see Refs. 134 and 157 for more details).

3.4. Formation of population wave as result of magnetotaxis of bacteria

At the beginning of the 1970s the young investigator Blakmore accidentally discovered that some bacteria can move along the lines of force of a magnetic field.[77,171–173] It turned out that magnetotaxis (i.e., the sensitivity to a mag-

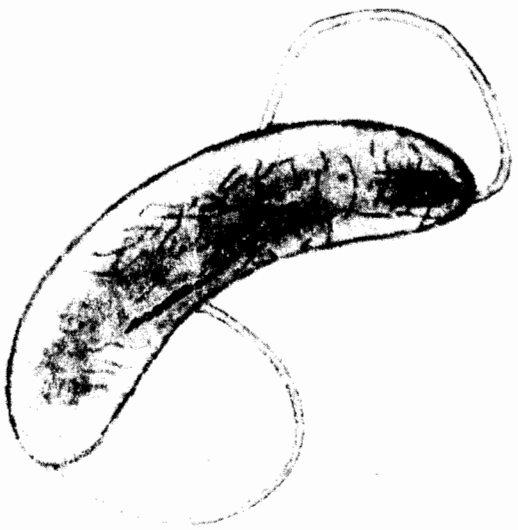

FIG. 15. Photograph of magnetotaxic bacteria.[172] Network of magnetosomes is visible.

netic field), typical for these organisms, is caused by chains of intracellular particles of magnetite (Fe_3O_4);[77,171-178] such particles are called magnetosomes (Fig. 15). These particle chains exhibit the properties of a magnetic dipole and behave similarly to a compass needle in the earth's magnetic field. As a result, the cells are oriented along the lines of force, and this is typical not only for living but also for dead cells.[173] The orientations of the cells prevent Brownian motion of the molecules of the culture medium in which the bacteria are living. The degree of orientation of the cells is characterized by the mean value of the cosine of the angle θ between the direction of the magnetic moment **M** of the cell and the direction of the external magnetic field **B**:

$$\langle \cos\theta \rangle = \frac{\int \cos\theta \exp(-E_m/kT)\, dV}{\int \exp(-E_m/kT)\, dV} = L(\alpha), \tag{63}$$

where $E_m = -MB\cos\theta$, k is the Boltzmann constant, T is the temperature of the medium over the volume of which the integration is performed. Here $L(\alpha)$ is the Langevin function: $L(\alpha) = \mathrm{cth}(\alpha) - (1/\alpha)$, $\alpha = MB/kT$. For $\alpha \geqslant 10$ we have $\langle \cos\theta \rangle \sim 1$, i.e., the cells must be almost completely oriented along the magnetic field. Measurements have shown[173,179-181] that $\alpha \sim 16$. Thus, in contrast, for example, to the *E. coli* bacteria magnetotactic bacteria move in a very ordered manner.[171-173] It was found that such ordered behavior can give rise to population waves.

The formation process and the subsequent propagation of these waves were first described in Refs. 182, 183. Two such waves are shown in Fig. 16. They appear as a result of a quasistatic hydrodynamic interaction between adjacent, parallel-oriented bacteria. The force acting on a bacterium is[184]

$$\mathbf{F} = \mathbf{F}_0 + \mathbf{F}^+, \tag{64}$$

where

$$\mathbf{F}_0 = -6\pi\mu a\mathbf{U}, \tag{65}$$

$$\mathbf{F}^+ = 6\pi\mu a[\mathbf{v}^\infty + \frac{a^2}{6\mu}(\nabla p^\infty)]. \tag{66}$$

In Eq. (64) $\mathbf{F}_0$ is the usual Stokes drag force imposed by the liquid, and is characterized by the dynamic viscosity μ, applied to a body moving with velocity **U** (see Eq. (65), where a is the characteristic size of the body). It is assumed here that the Reynolds number is $\mathrm{Re} \ll 1$, which, as pointed out

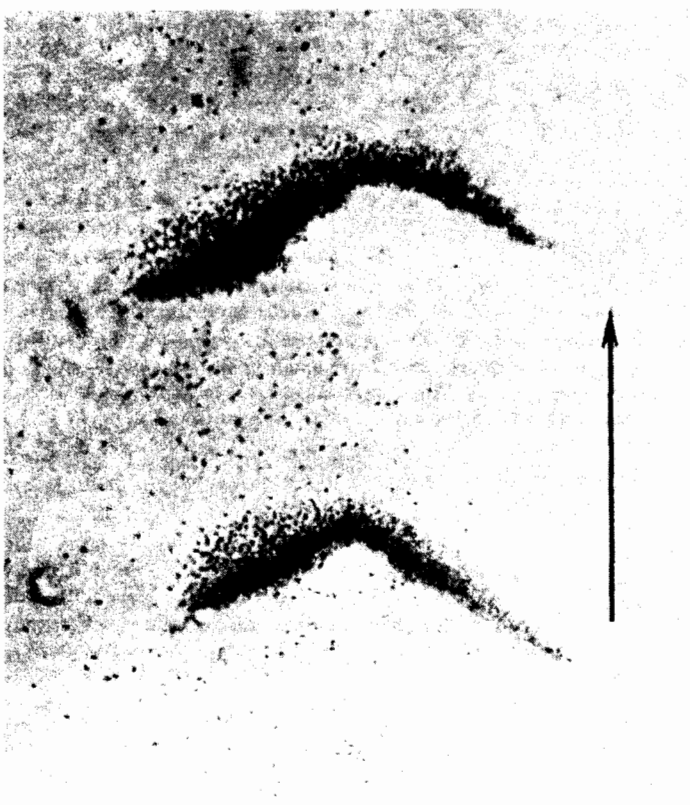

FIG. 16. Photograph of population waves, formed by magnetotaxic bacteria.[184] The waves moved along the lines of force of the magnetic field. Direction of motion is indicated by arrow.

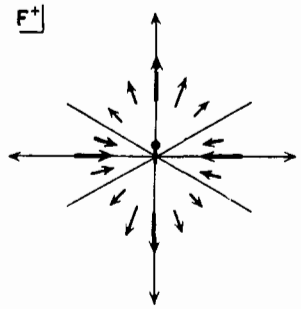

FIG. 17. Field of directions of the force $\mathbf{F}^+$, generated by the cell located at center of figure.[184]

above, is typical for the motion of bacteria. The quantity $\mathbf{F}^+$ is the auxiliary hydrodynamic force acting on one bacterium by another closely situated bacterium (the distance between cells must not exceed $\sim 10a$). In Eq. (66) $\mathbf{v}^\infty$ and p^∞ are, respectively, the unperturbed velocity and pressure fields of the liquid far from the interacting cells. As shown in Ref. 184, the force $\mathbf{F}^+$ can be defined in the following manner:

$$\mathbf{F}^+ = \hat{\mathbf{x}} \cdot \frac{9}{2} \pi \mu a U \frac{l^*}{a} \left(\frac{a}{r}\right)^2 \left[3\cos^2(\hat{\mathbf{u}}, \hat{\mathbf{x}}) - 1\right], \tag{67}$$

where $\hat{\mathbf{x}}$ is the unit vector, $\hat{\mathbf{u}} = \mathbf{U}/|\mathbf{U}|$, $(\hat{\mathbf{u}}, \hat{\mathbf{x}})$ is the angle between the vectors $\hat{\mathbf{u}}$ and $\hat{\mathbf{x}}$, r is the distance from the cell, $l^* = (1/2)(L + l_2)$, L is the distance from the front edge to the end of the flagellum propelling the bacterium, and l_2 is the distance between the two extreme points of the helical portion of this flagellum. The field of the directions of the force $\mathbf{F}^+$, generated by a cell located at the center of the figure, calculated from Eq. (67) is shown in Fig. 17. It is seen that the hydrodynamic interaction force causes a mutual attraction of parallel-oriented cells, swimming side by side. All of the rest of the bacteria repel one another. This character of interaction between the bacteria initiates population waves similar to those depicted in Fig. 16.

3.5. Spatial patterns caused by bioconvection

As early as 1848 it was known that many swimming micro-organisms can form spatial patterns on the surface of the culture medium that resemble Bénard convection cells (Fig. 18a).[185-190] It was suggested that these structures arise as a result of thermal instability. However, experiments did not bear out this hypothesis.[189] The most probable mechanism for their appearance is the Rayleigh–Taylor instability,[193] i.e., an instability of the upper layers of the culture medium as it fills with floating micro-organisms.[81] The reason for the floating (negative geotaxis) is apparently the positive taxis of the microbes to atmospheric oxygen, that is to say, oxytaxis.[191] As a result of the instability, downward-directed flows of micro-organisms (Fig. 18b) are formed, and bioconvection appears.

Actually, the upper layer of the culture medium enriched with micro-organisms can be considered as a liquid whose density exceeds the density of the lower layers.[80] From the incompressibility of a liquid[80] we obtain

$$\frac{\partial \rho}{\partial t} + u\frac{\partial \rho}{\partial x} + w\frac{\partial \rho}{\partial z} = 0. \tag{68}$$

In Eq. (68) we will restrict ourselves to a two-dimensional analysis, with ρ being the density of the liquid, u is the velocity of the micro-organisms in the x direction, and w is the velocity in the z direction. We will assume that the force of gravity acts along the z axis. We supplement Eq. (68) with the equation of continuity

$$\frac{\partial \rho}{\partial t} + \frac{\partial}{\partial x}(\rho u) + \frac{\partial}{\partial z}(\rho w) = 0. \tag{69}$$

Then it follows from Eqs. (68) and (69) that

$$\frac{\partial u}{\partial x} + \frac{\partial w}{\partial z} = 0. \tag{70}$$

We introduce the following notations:

$$p^* = p + p',$$

$$\rho^* = \rho + \rho',$$

where p and ρ are, respectively, the pressure and density of the liquid in the absence of bioconvection and p' and ρ' are small perturbations. In this case

$$\frac{dp}{dz} = -g\rho. \tag{71}$$

The linearized equations of motion in the x and z directions have the following form:[80]

$$\rho\frac{\partial u}{\partial t} = -\frac{\partial p'}{\partial x}, \tag{72}$$

$$\rho\frac{\partial w}{\partial t} = -\frac{\partial p'}{\partial x} - g\rho'. \tag{73}$$

Equation (68) in linearized form is

$$\frac{\partial \rho'}{\partial t} + w\frac{\partial \rho}{\partial z} = 0. \tag{74}$$

Assuming that the dependences of ρ', p', u and w on x and t have the form $\exp(nt + ikx)$, we obtain from Eqs. (74), (70), (72) and (73), respectively,

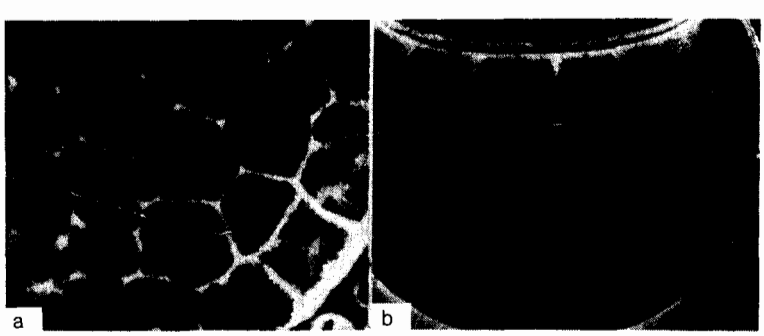

FIG. 18. Spatial patterns appearing as a result of bioconvection in culture of micro-organisms (*Tetrahymena pyriformis* infusoria in this case).[81] a–Top view, b–Side view.

$$n\rho' + w\frac{d\rho}{dz} = 0, \tag{75}$$

$$iku + w_z = 0, \tag{76}$$

$$n\rho u + ikp' = 0, \tag{77}$$

$$n\rho w + p_z' + g\rho' = 0. \tag{78}$$

In Eqs. (75)–(78) $w_z = dw/dz, p_z' = dp'/dz$. It follows from Eqs. (76) and (77) that

$$-p' = \frac{n\rho w_z}{k^2},$$

and from Eqs. (75) and (78)

$$-p_z' = n\rho w - \frac{g}{n}\rho_z w.$$

Eliminating p' from the last two equations, we obtain

$$w_{zz} + \beta w_z - wk^2\left(1 - \frac{g\beta}{n^2}\right) = 0, \tag{79}$$

where $\beta = \rho_z/\rho$, $\beta = \text{const}$ (this is true if, for example, $\rho(z) = \rho_0 e^{\beta z}$). The solution of Eq. (79) has the form[80]

$$w = e^{ikx+nt}(Ae^{m_1 z} + Be^{m_2 z}),$$

where

$$m_1 = 1/2\cdot\{-\beta + [\beta^2 + 4k^2(1 - g\beta/n^2)]^{1/2}\}, \tag{80}$$

$$m_2 = 1/2\cdot\{-\beta - [\beta^2 + 4k^2(1 - g\beta/n^2)]^{1/2}\}. \tag{81}$$

If $w = 0$ for $z = 0$, then

$$w = Ae^{ikx+nt}(e^{m_1 z} - e^{m_2 z}).$$

It can be shown[80] that at the upper boundary of the liquid (for $z = d$) a reasonable boundary condition is

$$w = 0.$$

Then

$$\exp[(m_1 - m_2)d] = 1,$$

or

$$(m_1 - m_2)d = 2il\pi, \tag{82}$$

where l is an integer. It follows from Eqs. (80)–(82) that

$$n^2 = \frac{g\beta k^2 d^2}{k^2 d^2 + (1/4)\beta^2 d^2 + l^2\pi^2}, \tag{83}$$

where $l = 1, 2, 3,\ldots$ We exclude $l = 0$ from consideration since for $l = 0$ $w = 0$ for all values of z.

With the viscosity taken into consideration Eq. (83) is replaced by the following equation (for $l = 1$):[194]

$$n^2 + 2\nu k^2 n - \frac{g\beta k^2 d^2}{k^2 d^2 + (1/4)\beta^2 d^2 + \pi^2} = 0,$$

where ν is the kinematic viscosity. For $k' = kd$, $\beta' = \beta d$, $n' = n/(\beta g)^{1/2}$, $\nu' = \nu/d^2(\beta g)^{1/2}$ this equation assumes the following form:

$$n'^2 + 2\nu'^2 k'^2 n' - \frac{k'^2}{k'^2 + (1/4)\beta'^2 + \pi^2} = 0. \tag{84}$$

For the parameter values $d = 1$ cm, $\beta = 5.9\times 10^{-5}$ cm^{-1}, $g = 10^3$ cm/s^2 and $\nu = 0.01$ cm^2/s, $n'(k')$ has a maximum[80] at $k' = 4$. This value of k' corresponds to a wavelength $\lambda = 1.6$ cm. The typical size of the cells appearing in the surface layer in the presence of bioconvection is close to this value of λ.[81]

3.6. Spatial patterns appearing as a result of gyrotaxis of micro-organisms

Negative geotaxis, i.e., preferred motion of micro-organisms opposite to the direction of the force of gravity, can also be caused by other factors besides oxytaxis.[191] One of these is associated with the noncoincidence of the center of mass with the geometrical center of micro-organisms (such as the *Chlamydomonas* or *Dunaliella* cells,[82,195,196]). This noncoincidence can be caused by an asymmetric localization of the cell organella. A conventional picture of a spheroidal cell is depicted in Fig. 19a. The radius of such a cell is usually 3–5 μm and its velocity[196] is $v_c \leqslant 200$ μm/s. The displacement of the center of mass with respect to the center of the sphere is given by the vector **L** (see Fig. 19a). The torque caused by this displacement is equal to $\mathbf{L}\times\mathbf{g} = \varphi mgL\sin\theta$, where $\mathbf{g} = -g\hat{\mathbf{z}}$, $\hat{\varphi} = \hat{\mathbf{z}}\times\hat{\mathbf{r}}$, $\hat{\mathbf{r}}$, $\hat{\varphi}$ and $\hat{\mathbf{z}}$ are unit vectors. As is known,[197] a body immersed in a liquid flow is subject a hydrodynamic torque resulting from the gradient of the liquid

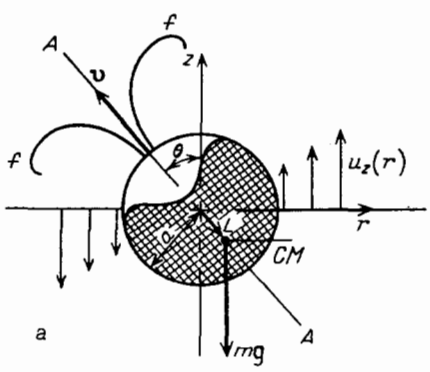

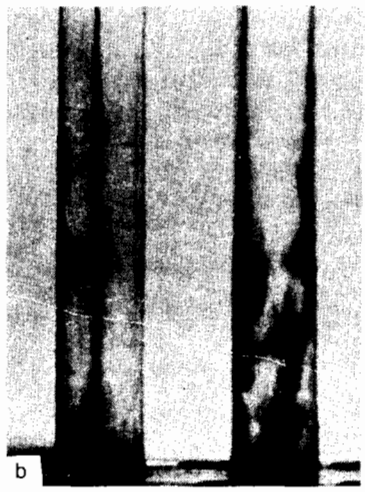

FIG. 19. a–Idealized spherical cell in a liquid medium moving with respect to it.[196] $U_z(r)$ is the relative velocity of the liquid. The flagella (f) move the cell in the direction AA with a velocity v. The gravitational force produces a torque, numerically equal to mgL sin θ; CM is the center of mass. b–Focusing of freely swimming *Chlamydomonas nivalis* micro-organisms, caused by gyrotaxis.[196] In the left cylinder, where the liquid flow was downward, cells accumulated near the cylinder axis; in the right cylinder, where the liquid flow was upward, the cells moved out to the periphery.

velocity $\mathbf{u}(\hat{\mathbf{r}})$. The hydrodynamic and gravitational torques add together, yielding

$$\mathbf{T} = 8\pi\mu a^3\left(\frac{1}{2}(\nabla\times\mathbf{u}) - \omega\right) + m\mathbf{L}\times\mathbf{g},$$

where ω is the angular rotation velocity of the sphere, $\nabla\times\mathbf{u}$ is the vorticity, and μ is the viscosity. The influence of the motion of the flagella is assumed to be negligibly small.[196] When $\mathbf{u} = u(r)\hat{\mathbf{z}}$ (see Fig. 19a), the condition $\mathbf{T} = 0$ yields

$$\sin\theta = \beta/v_c(\nabla\times\mathbf{u})_\varphi, \tag{85}$$

where the gyrotactic scale is $\beta = 4\pi\mu a^3 v_c/mgL$. For $a = 4$ μm, $v_c = 200$ μm/s and $L = 0.03a$, we have $\beta = 0.05$ cm.

If the downward vertical flow of liquid is bounded by a cylinder of radius R, then

$$\mathbf{u}(\mathbf{r}) = -u_0(1 - r^2/R^2)\hat{z},$$

and therefore

$$v_c\sin\theta = 2u_0 r\beta/R^2.$$

In the laboratory reference system the velocity of a cell is

$$\mathbf{c} = -(v_c\sin\theta)\hat{\mathbf{r}} + [v_c\cos\theta - u_0(1 - r^2/R^2)]\hat{\mathbf{z}}. \tag{86}$$

A principal conclusion from Eq. (86) is that even in the absence of a liquid flow ($u_0 = 0$) the cells are oriented with the flagella upward (as in the diagram shown in Fig. 19a); in this situation they float (their style of swimming resembles the breast stroke). The directed motion of the micro-organisms against the force of gravity (negative geotaxis) in this case is not due to the operation of any set of cell tools specially adapted for this (which is necessary, for example, for chemotaxis exhibited by the *E. coli* bacteria). The cells simply continue to swim in the direction in which they are oriented by virtue of their intrinsic asymmetry.

As a result of this directed motion the cells accumulate in the upper layer of the culture medium. When their concentration exceeds some threshold value, bioconvection occurs in accordance with the Rayleigh–Taylor mechanism. In this situation spatial patterns appear similar to those[82] depicted in Fig. 18. Thus, the cell structures characterizing the distribution of micro-organisms in the upper layer of the culture medium are caused necessarily by chemotaxis.

Under bioconvection conditions flows arise, not only of micro-organisms, but also of the liquid that is their culture medium. Let us assume the characteristic radius of such a flow is R. Then in accordance with Eqs. (85) and (86) the cells will swim upward, opposite to the downward flow and at the same time they will be constrained to central axis of the downward flow. If the flow is upward, the signs of u_0 and $\nabla\times\mathbf{u}$ are reversed. Consequently, as seen from Eq. (85), the sign of $\sin\theta$ is also reversed. This means that in the upward direction the stream of cells must deviate from the axis and accumulate around the periphery of the flow. Experiments completely confirm these conclusions (see Fig. 19b).

Gyrotaxis is the directed motion of cells caused by a compensation of the torques caused by outside forces. Such motion, as shown in Fig. 19b, can cause a spatially inhomogeneous distribution of micro-organisms.

Let us consider more carefully the situation when the liquid flow is downward (in Fig. 19b this situation is depicted in the left cylinder). In this situation the swimming (with respect to the liquid) cells are constrained to the axis of the cylinder. Because of the increase in cell concentration near the axis of the cylinder the velocity of the flow increases in the immediate vicinity of the axis. Since the quantity $(\nabla\times\mathbf{u})_\varphi$ also increases in this situation, $\sin\theta$ must also increase in accordance with Eq. (85). It is clear from Fig. 19a that this leads to an acceleration of the accumulation of cells around the axis of the flow (in Fig. 19a the angle θ is measured counterclockwise). Such an acceleration causes a further increase in the flow velocity, and so forth. In this situation the radius of the flow decreases and its boundaries become sharper. Such a gyrotaxis-caused self-focusing of algae cells is called a "green hole" (by obvious analogy to "black holes").[82]

Thus, swimming cells (as a result of Rayleigh–Taylor type instabilities) can form downward flows of liquid and cells, cell convection appears, and the downward flows are transformed into "green holes". These effects are caused by gyrotaxis.

To conclude this section let us mention that the phenomenon of gyrotaxis has been examined in greater detail in Refs. 198–201.

3.7. Spatial patterns appearing as a result of the interaction of converging population waves formed by chemotactic bacteria

It was shown above (Sect. 2.1) that mobile bacteria (e.g., *E. coli*), planted in a semiliquid culture medium, can form fronts characterized by an elevated density of microorganisms.[59,116,118–121] The migration of these fronts can be considered as a propagation of an autowave and it can be described by typical "reaction-diffusion" type autowave equations.[122,123,125,127,139–141,145,154,202]

The simultaneous planting of bacteria at several points of one Petrie dish leads to the interaction of the converging fronts (also called chemotaxis rings).

The chemotaxis rings can suffer collisions, such as the one shown in Fig. 20. Sometimes the population waves can pass through each other.[203] In this situation, as was shown in 1990 by Shakhbazyan, the bacteria can switch from the consumption of one substrate (before the moment of collision) to the consumption of the other, and in this way the waves penetrate through each other.

FIG. 20. Collision of chemotaxis rings.[119] Three population waves are leaving each inoculation point in succession. The first wave consists of bacteria demonstrating positive taxis with respect to serine (and consuming it), the second wave demonstrates taxis to aspartate, and the third to threonine.

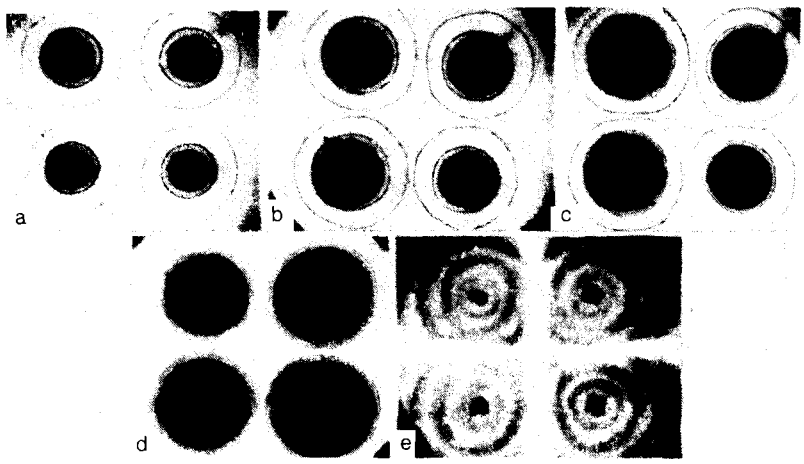

FIG. 21. Appearance of noncolliding pattern when chemotaxis rings converge.[9] a–Two expanding (from inoculation points) chemotaxis rings. b, c–Retardation, deformation of rings, formation of cross-shaped pattern as rings converge; individual bacterial populations are separated by planar demarcation zones. d–Second chemotaxis rings cannot cross demarcation zones. e–Growing (following the chemotaxis rings) bacterial lawns also do not cross the demarcation zones, which form a stationary structure; it is seen that typical stationary rings (not chemotaxis rings), formed by the bacterial lawn, are "torn" at this structure.

However, chemotaxis rings do not always collide. In some cases they slow down and stop as they approach each other, without coming into direct contact.[9,204–206] The successive stages of this process are demonstrated in Fig. 21. It is seen that the rings, coming together, are deformed (the curvature of the front is reduced locally). Then the chemotaxis rings slow down and stop (without colliding). A spatial pattern of four bacterial populations is formed, separated by a cross-shaped demarcation zone. This pattern is preserved for a long time (more than 10 hours after collision).

It turned out that the type of structure—colliding (as in Fig. 20, for example) or noncolliding (Fig. 21)—is determined by the expansion velocities of the chemotaxis rings.[9] No collision of the waves occurs when their average velocity does not exceed ~ 4 mm/h.

The assumption has been made that the appearance of the noncolliding patterns is due to a shortage of the culture substrate (which is an attractant at the same time) in front of the slowly moving population waves.[9] In the narrow demarcation zones, separating the individual populations (Fig. 21), this shortage can evidently play a key role in the formation of the noncolliding structures. A mathematical modeling that we carried out for the interaction processes of converging population waves demonstrated the soundness of this assumption.

A modified system of the Lapidus–Schiller system of equations was used as the mathematical model:[207]

$$\frac{\partial b}{\partial t} = R(s)b + D_b \frac{\partial^2 b}{\partial x^2} - V \frac{\partial}{\partial x}\left(b \frac{\partial f(s)}{\partial x}\right), \tag{87}$$

$$\frac{\partial s}{\partial t} = -\lambda(s)b + D_s \frac{\partial^2 s}{\partial x^2}, \tag{88}$$

where in contrast to the original model,[207] λ (as in Ref. 208) is not a constant: we assumed that $\lambda(s) = \alpha R(s)$, $\alpha = \text{const}$ ($\alpha \leqslant 1$). The quantity b is the concentration of bacteria and s is the density of the substrate,

$$R(s) = R_0 s(s + s_k)^{-1}, \quad R_0 = \text{const}, \quad s_k = \text{const},$$
$$f(s) = s(s + s_k)^{-1}. \tag{89}$$

The initial conditions were specified in the following manner:

$$b(x, t = 0) = \begin{cases} b_0 \text{ for } 0 \leq x \leq \text{and} (L - \varepsilon) \leq x \leq L, \\ 0 \text{ for rest of } x \text{ coordinate values,} \end{cases}$$

where L is the distance between the "backs", i.e., the boundaries of the initial bacteria concentration regions facing away from each other (ε is the characteristic size of these regions),

$$s(x, t = 0) = s_0.$$

The first term on the right side of Eq. (87) describes the multiplication of bacteria, and the multiplication rate R depends on the density of the culture substrate s at a given point of the medium. The presence of this term is a major distinction between the mathematical model (87) and (88) and the Keller–Segel model (18), (19). The second term on the right side of Eq. (87) describes the random walk of the bacteria (D_b is the diffusion constant assumed to be a constant), and the third term is the gradient of the bacteria flux caused by chemotaxis. Unlike in the Keller–Segel model[122], this flow in the Lapidus–Schiller model[207] depends not on the gradient of the substrate, $\partial s/\partial x$, but on $\partial f/\partial x$, where the function $f(s)$, given by Eq. (89), is the so-called sensitivity function of the bacteria to a given substrate (which is simultaneously an attractant). This approach agrees better with existing experimental data.[98] The second equation of the mathematical model being analyzed (Eq. (88)) describes the change in the concentration of the attractant (or substrate); here D_s is the diffusion constant of the substrate. The one-dimensional case is considered in Eqs. (87) and (88) for simplicity.

Computer experiments that we have performed have shown that the noncolliding patterns arise in those cases when the parameter V in Eq. (87) is not very large ($V \leqslant 1$), or, in other words, when the nonuniformities caused by chemotaxis in the bacteria concentration (i.e., the population waves) are not propagating too fast. This result agrees qualitatively with the data obtained in Ref. 9.

Figure 22 shows the successive stages of formation of the noncolliding structure, along with the associated substrate distributions. It is seen that in the concluding stage the substrate concentration in the gap between the arrested population waves decreases to zero. Thus, the noncolliding pattern can be formed as a result of the eating out of the substrate in the space between the two converging population waves (if the rate of their convergence is not too large).

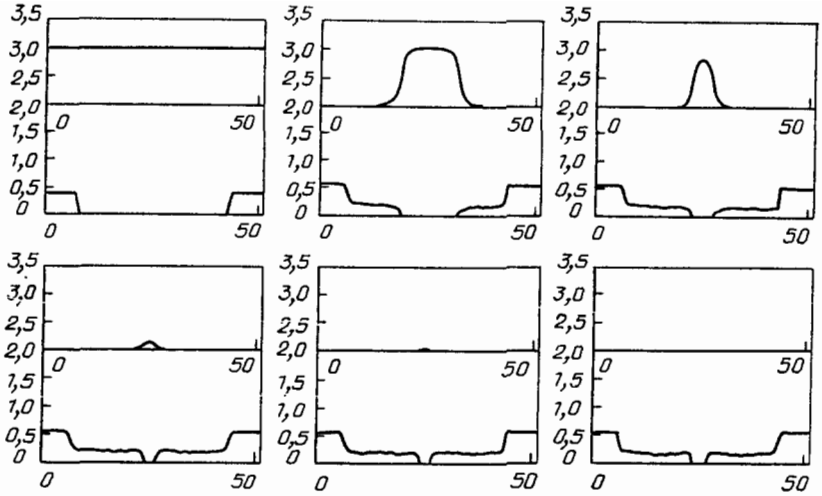

FIG. 22. Successive stages in formation of noncolliding pattern. Each of the six stages shown in the upper graph represent the $s(x)$ dependence, those in the lower $b(x)$.

This conclusion is also confirmed in natural experiments, where the chemotaxis rings propagated and converged in a synthetic culture medium. This medium contained only one substrate (attractant), for example, D-glucose. The results of these experiments are shown in Fig. 23. It is clearly seen that the concentration of D-glucose in the demarcation zone formed by the two converging bacterial rings falls off sharply from its initial value. Whereas the initial concentration of the attractant (in different experiments) ranged from 0.67 to 1.46 μM/ml, in the demarcation zone it decreased to values of 0–0.16 μM/ml.

An interesting result is that the demarcation zones are preserved for a period of 10 hours and they do not vanish as a result of the intrinsic diffusion of the bacteria.[9] This is easily explained by the dependence of the bacteria mobility on the substrate concentration. As an example, it was assumed in Ref. 231 that the mobility is

$$\mu(c) = \begin{cases} \mu_0 (ac)^n & \text{for } c \leq 1/a, \\ \mu_0 & \text{for } c > 1/a, \end{cases}$$

where a and n are non-negative constants. It can be seen that $\mu(c)$ can decrease considerably with a decrease in c. The demarcation zones in this case are obviously stabilized. Products of metabolism, inhibiting the mobility of bacteria,[9] may play some role in the stabilization of these zones.

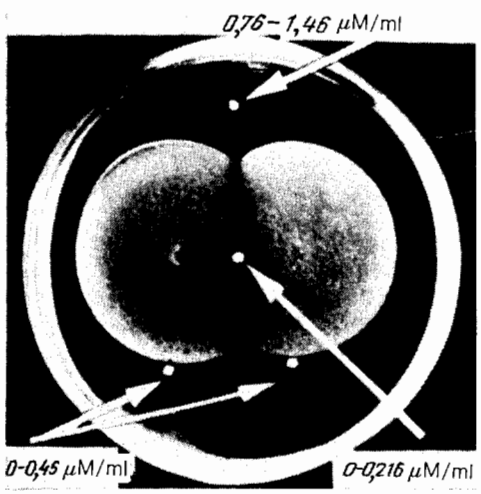

FIG. 23. Decrease in concentration of D-glucose in culture medium during formation of noncolliding population pattern. Arrows indicate the sites where samples were taken to measure the concentration of D-glucose: far from the converging waves (control sample), in the immediate vicinity of front of leading wave, and in demarcation zone.

3.8. Spatial patterns associated with an instability of the regular geometrical shape of chemotaxis rings

We have seen that bacterial population waves (if they do not interact) usually have a regular geometrical shape, such as that of a ring (as in Fig. 11). However, this shape is not always stable during propagation of a population.

In some cases, as shown in our experiments,[209] the regular shape of a chemotaxis ring is destroyed when it reaches some critical radius (R_{cr}). In this situation bulges are thrown out in the form of segments, separated from the original bacterial population by gaps (Fig. 24). The number of these bulges usually varies from three to five. In turn, these segments often formed secondary bulges. The value of R_{cr} depends on the pH of the culture medium. Specifically, R_{cr} decreases monotonically (by a factor of about two) with an increase in pH from 4 to 8.

The mechanism for the formation of patterns such as that shown in Fig. 24 is not yet clear. One can suppose that the breakup of the geometrical shape of the chemotaxis rings is caused by a buildup of a repellent or repellents, which are a product of the vital activity of the bacteria. Bulges can be formed when the repellent concentration reaches some

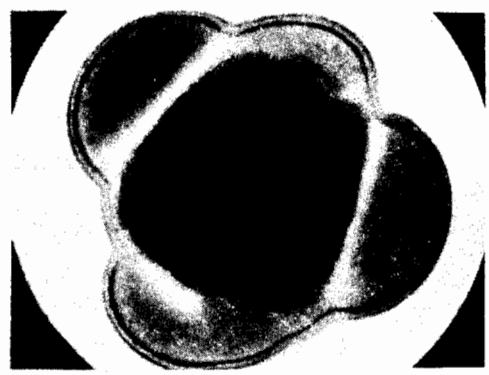

FIG. 24. Spatial bacterial pattern formed as a result of instability of regular geometrical shape of chemotaxis ring, formed by *E. coli* bacteria.

threshold value; in this case the radius of the chemotaxis rings reaches the value of R_{cr}. The formation of the bulges is due to a drift of the bacteria opposite to the gradient of the repellent from its region of maximum concentration, which obviously coincide with the chemotaxis ring and characterized by an increased density of bacteria. The appearance of bulges is determined (within the framework of this hypothesis) by fluctuations of the repellent gradient. The width of the gaps separating the segment-shaped bulges from the original population (see Fig. 24) may depend on the maximum value of the repellent gradient, at which the directed motion of bacteria opposite to this gradient vanishes.

3.9. Spatial patterns appearing as the result of an interaction of bacteria and viruses

The name "virus" (from the Latin meaning poison) was first used to designate various little-studied pathogenic agents. Later, it was assigned to a group of pathogens discovered in 1892 by Ivanovskiĭ, which turned out to be able to pass through bacterial filters.[21] Viruses differ from microorganisms in the following respects: 1) they contain only one type of nucleic acid—either DNA or RNA; 2) only nucleic acid is required for their reproduction; 3) they are unable to multiply outside a living cell (see, e.g., Refs. 21, 210). Thus, viruses are not independent organisms, but utilize living cells for their multiplication: their reproduction occurs in a host cell. Cell mechanisms are needed both for replication of the nucleic acid and also for synthesizing the protein membrane of the virus. Growth of the virus leads to death of the host cell. Outside the cell a virus exists in the form of a virus particle (virion), which consists of the nucleic acid and protein membrane-capsid.

Viruses that are harmful to bacteria are called bacteriophages. Bacteriophages are identified from the formation of so-called "sterile spots" or "blotches", in a solid bacterial lawn (Fig. 25). Cell lysis is accompanied by the evolution of the newly formed virions in the culture medium.

It is clear from Fig. 25 that the morphology of the blotches may be determined by the type of phage. In particular, some bacteriophages produce blotches surrounded by a halo (for example, the T3 phage; Fig. 25). A possible mechanism for the formation of the halo was suggested in Ref. 212. In that paper it was shown that the cells being dissolved can form an enzyme, which blocks further lysis. In a region where the concentration of this enzyme is sufficiently high, the lysis is retarded and a halo is formed. Further formation of the enzyme is also reduced in this case. This causes the appearance of another ring-shaped lysis zone surrounding the halo (as in the action of the T3 phage in Fig. 25); target-like blotches appear. Sometimes they have a rather complex multiring structure.

An analysis of this model showed, however, that it must be supplemented.[214] That is, the formation of the target-like blotches of sterility must include the transport of the adsorbed phages by a stream of the cells being dissolved (during the transport process), this stream appearing as a result of a negative chemotaxis of these cells in the substances formed in the culture medium in the zone of active lysis. An appropriate mathematical model has been suggested by one of the authors of this review (Tsyganov). It is the system of equations

$$\partial b/\partial t = \mu(s)b - \eta b + D_b\nabla^2 b + VQ(h)\nabla(b\nabla Q(h)), \quad (90)$$

$$\partial p/\partial t = N\eta b - kbp + D_p\nabla^2 p, \quad (91)$$

$$\partial p_a/\partial t = kbp - \eta p_a + VQ(h)\nabla(p_a\nabla Q(h)), \quad (92)$$

$$\partial h/\partial t = \alpha\eta b + D_h\nabla^2 h, \quad (93)$$

$$\partial s/\partial t = -\beta(s)b. \quad (94)$$

In Eqs. (90)–(94) b is the bacteria concentration, p is the density of virions, p_a is the mean density of bacteriophages adsorbed on the bacteria, h and s are, respectively, the concentration of the enzyme inhibitor of the lysis and the concentration of the substrate. Equation (90) describes the change in bacteria concentration with time due to the following processes: 1) multiplication (μ is the specific rate of

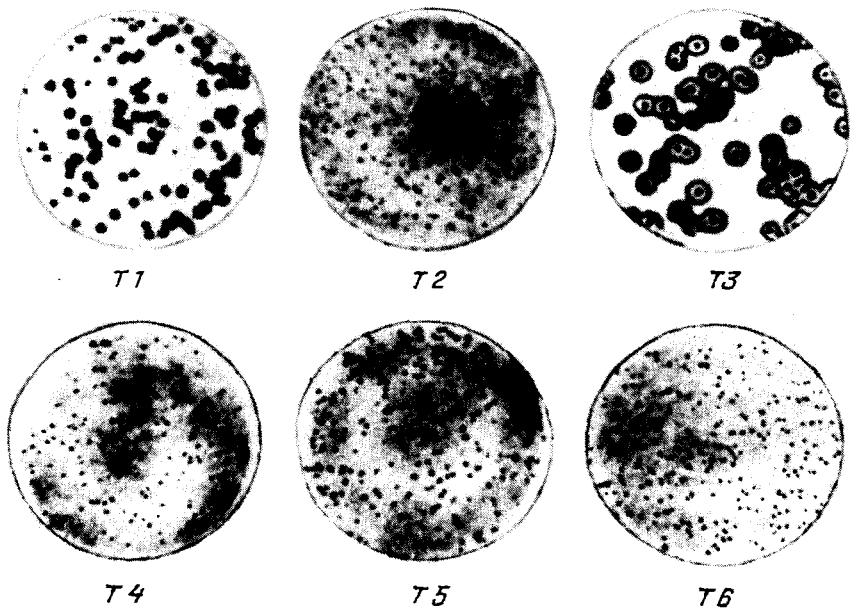

FIG. 25. Blotches formed by six different types of phages in continuous lawn of *E. coli* bacteria.[211]

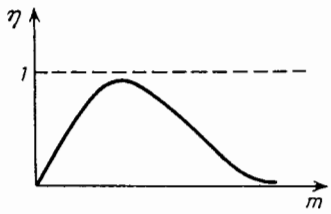

FIG. 26. The function $\eta(m)$ in the Tsyganov mathematical model (Eqs. (90)–(94).

growth of the number of bacteria); 2) lysis ($\eta(m)_0$ is the specific lysis rate, where the multiplicity $m = p_a/b$ has the form shown in Fig. 26); 3) diffusion (D_b is the diffusion constant) and 4) negative taxis of bacteria in the lysis zone; here $Q(h) = h/(h + h_k)$, where h_k is a constant and $V = \text{const}$ determines the strength of the chemotactic response of the bacteria. Equation (91) describes the change in the concentrations of virions with time due to the following processes: 1) the yield of virions from the dying cells (N is the average yield of virions in the lysis of one bacterium); 2) bonding of phages with cells (k is the binding constant) and 3) diffusion of virions (D_p is their diffusion constant). Equation (92) describes the change in the concentration of phages bound to cells still undissolved. It is assumed that the cells, leaving the lysis zone (because of negative chemotaxis), carry bound bacteriophages with them—the source of their future death. This process is described by the third term on the right side of Eq. (92).

Equation (93) relates the change in the lysis enzyme-inhibitor to the concentration of the cells being dissolved (α is a constant) and to the diffusion of this enzyme (D_h is the diffusion constant). Finally, Eq. (94) describes the change in the substrate concentration due to its consumption by the bacteria (β is the specific rate of consumption; it depends on the substrate concentration in the same manner as the function $\lambda(b)$ in the modified Lapidus–Schiller model; see Eqs. (87) and (88)). The Tsyganov model makes it possible to analyze the formation process of the target-like sterility blotches.[213]

Figure 27a shows an example of a computer experiment performed on the basis of this model. The evolution of the target-like blotches, recorded in the course of a natural experiment (infection of an *E. coli* bacterial lawn by the T7

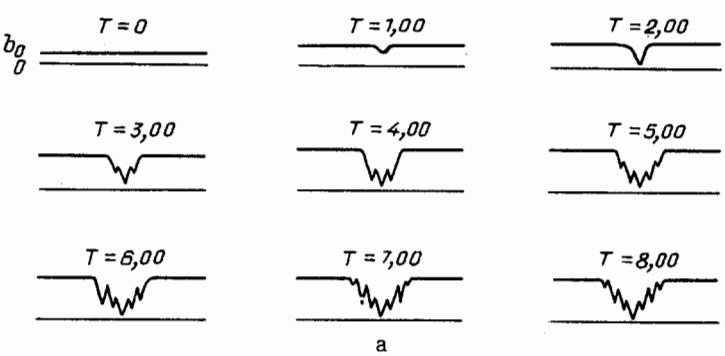

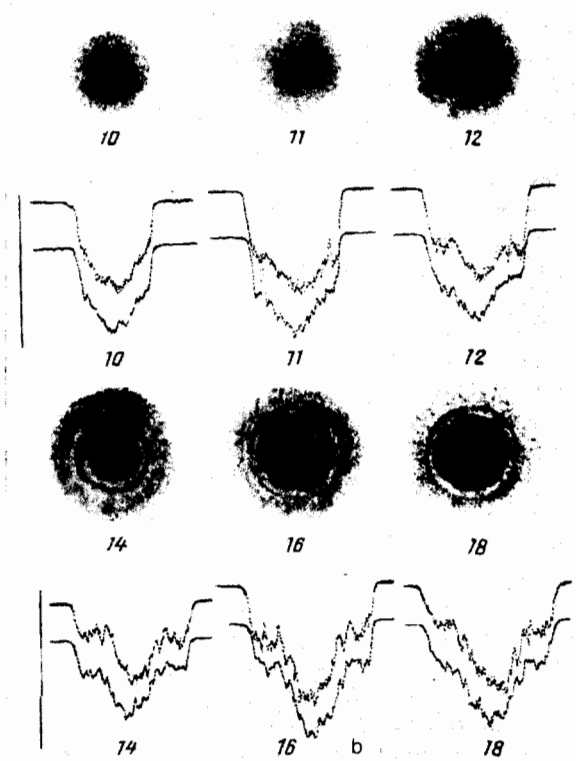

FIG. 27. a–Numerical modeling of the formation of target-like patterns, based on Eqs. (90)–(94). b–Evolution of sterility blotches (*E. coli* bacteria and T7 bacteriophage). Spatial patterns are shown together with the variation of their optical density in two mutually perpendicular directions.

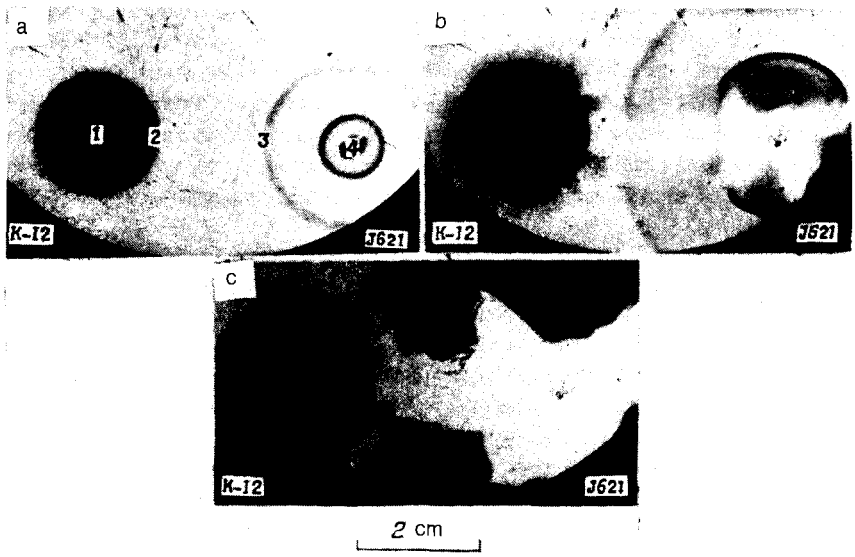

FIG. 28. Result of the action of T7 bacteriophage on the spatial patterns formed by the J621 and K-12 strains.[217] a–Pattern at moment of infection; 1–4–points of infection. b–Pattern 2.5 hours after infection. c–Pattern 5 hours after infection.

phage), is shown in Fig. 27b. It is seen that the computer experiment reproduces well the basic features of the formation process of these blotches.

Let us consider yet another way that spatial patterns are formed during the interaction of phages with bacteria. It is known that a phage infection is sometimes accompanied by incomplete lysis. This may be due to the presence of phage-resistant cells in the population.[210,215] However, even in the absence of such cells conditions exist for which a spatially distributed population of bacteria can survive despite a virus infection.[216,217] The result of the effect of the T7 phage on spatial patterns, formed by two different strains of bacteria, J621 and K-12, is demonstrated in Fig. 28. Figure 28a shows the points at which the phage infection was applied. The results of the infection are shown in Figs. 28b and 28c. It is seen that at the end of 5 hours the population of the J621 strain has essentially perished. At the same time the K-12 population is almost unaffected by lysis: the action of the phage is restricted just to a region near the point of the initial infection, not extending far along the chemotaxis front nor into the depth of the expanding bacterial population (compare Figs. 28b and 28c). As a result the population of the K-12 strain survives as a whole, resisting the bacteriophage infection. What is the mechanism for this survival?

It is known that phage lysis is possible in growing bacterial populations.[218] As shown in Ref. 217, the duration of the growth phase of the J621 strain is much longer than it is for K-12: 200 min after the beginning of measurements the growth of the K-12 population is drastically slowed down, whereas the population of the J621 strain continues to add to its density. Therefore, with the infection of the K-12 bacterial culture with the bacteriophage in the late stages of its growth phase the culture is able to leave this phase before the phage starts to affect it. There is no lysis in this case. On the other hand, the J621 culture is growing and is subject to lysis throughout the entire time of the experiment, i.e., when different bacterial populations are infected simultaneously, the one in which the duration of the growth phase is shorter is more resistant to lysis.

Since a local lysis occurs in the population of the K-12 strain only at the front near the point of infection, immediately behind the front this population is outside the growth phase. That is, the duration T of the growth phase and the average rate (V) of expansion of the chemotaxis ring are such that only a narrow ring adjacent to the front is subject to lysis. In the case presented $V \sim 1.5$ mm/h and $T \sim 3$ h; consequently, the width Δl of this ring must be about 4.5 mm, which agrees with the experimental data (see Fig. 28).[217] For J621 $V \sim 5$ mm/h (see Ref. 9 also) and $T \sim 5$ h; consequently, $\Delta l \sim 25$ mm which nearly coincides with the radius of the annular front of the chemotaxis (see Fig. 28).

The dependence of the survival of a multicell system on the life phase is not a specific feature of the interrelationships of phages with bacteria. It is interesting to note that the idea of the possible consequences of the infection of a man by a phase-dependent virus was used in a fantasy novel by Merle:[219] the author suggested that a disease pathogen can kill men in the reproductive period of their life. It is important, however, that a phase-dependent character of the action of a parasite on a host is also true in real situations. For example, the early development stage of insects has a less-developed protective response to endoparasites[220] (other examples can be found in the monograph[221]).

3.10. Spatial patterns that appear as a result of the interaction of converging bacterial population waves and that depend on the sex of the bacteria

As far back as the mid-1940s it was shown that bacteria can engage in their own unique kind of mating. Genetic material is transferred from the donor ("male" strain) to the recipient ("female" strain). Sexual differences of bacteria are caused by the so-called F factor (from the English word fertility). Cells, not containing the F factor (F^- cells) can function only as recipients. Donor cells have been given the name Hfr (see, for example, Ref. 21).

It has been shown[222] that both Hfr as well as F^- strains of the *S. typhimurium* bacteria can form chemotaxis rings. It was found that the spatial patterns, caused by the convergence of Hfr and F^- annular fronts, have an interesting feature. As seen from Fig. 29, Hfr bacteria have formed in the contact zone of two populations an arc-shaped wave, penetrating to some distance into the population of F^- cells. It is suggested that positive chemotaxis of Hfr bacteria in some hypothetical metabolite, evolved by the F^- cells, may be the

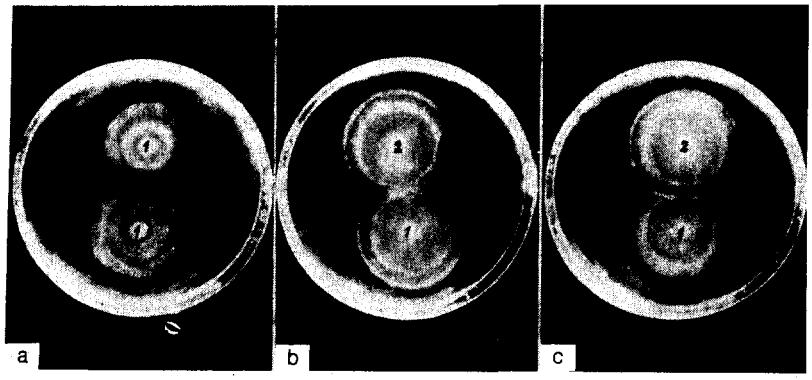

FIG. 29. Spatial patterns that appear as the result of the action of converging chemotaxis waves and that depend on the sex of the bacteria.[222] *1*–point of inoculation of F^- strain of *S. typhimurium* bacteria, *2*–point of inoculation of Hfr-strain.

basis of the mechanism for the appearance of such a spatial pattern.[222]

3.11. Effect of the age heterogeneity of populations on the spatial pattern

In certain cases the age heterogeneity of populations exerts a key influence on their fate. We became convinced of this while studying the survival of expanding bacteria populations in the presence of a local virus infection (see Sect. 3.9): it was found that survival is determined by the degree of spatial heterogeneity of the cell collectives relative to the growth phase.[217] Other effects may also be associated with age heterogeneity, for example, the appearance of pulsations in the spatial distribution of the number of dividing organisms. In order to show this it is sufficient to add a diffusion term to the equation of dynamics of the age makeup of a population:[224]

$$\frac{\partial n}{\partial t} + \frac{\partial n}{\partial \tau} = -\alpha(\tau)n + \operatorname{div}(D \operatorname{grad}(n)), \tag{95}$$

where t is the time, τ is the age, $n(t, \tau, x, y)$ is the age density of the population, x and y are spatial variables, $\alpha(\tau)$ is the mortality coefficient, and D is the diffusion constant of the organisms. Equation (95) must satisfy the following conditions:

$$n(t, 0, x, y) = \int_0^\infty b(\tau)n(t, \tau, x, y)\mathrm{d}\tau,$$

$$n(0, \tau, x, y) = \varphi(\tau, x, y),$$

where $b(\tau)$ is the birth rate coefficient and $\varphi(\tau, x, y)$ is the initial age distribution of the population in space.

Let us consider the development process of a population initially synchronous and located at a single point:

$$\varphi(\tau, x, y) = N_0\delta(x, y)\delta(\tau - \tau_0), \tag{96}$$

where N_0 is the initial population count, and δ is the Dirac delta function. For $D = \text{const}$ (see Eq. (95)) no spatially nonuniform patterns appear.[224] In order for them to appear it is necessary to impose additional conditions (which follow from the biological aspect of the problem). As an example, one can assume that the mobility of species depends not only on their count but also on their age. For the *E. coli* bacteria such a dependence was successfully demonstrated experimentally.[225,226] It was suggested in Ref. 224 that the diffusion constant D increases with an increase in the population of organisms, and their mobility is maintained constant only within some interval of age, i.e., in a certain phase of development. With these assumptions the appearance of spatially nonuniform distributions in population becomes possible. Figure 30 shows an example of the development of an initially synchronous point population in space (i.e., satisfying condition (96)). It was assumed here that

$$D = H(N - N^*)H(\tau^* - \tau), \tag{97}$$

where

$$N = \int_0^\infty n(\tau, x, y)\mathrm{d}\tau,$$

H is the Heaviside step function and N^* and τ^* are the critical number of individuals and the critical age, respectively. An interesting point is that the evolution of the spatial distribution shown in Fig. 30 reproduces well the spatial nonuniformity in population and the growth of cities, where the population density per unit ground area fluctuates from the center to the periphery.[224]

For the *E. coli* bacteria the dependence of the mobility

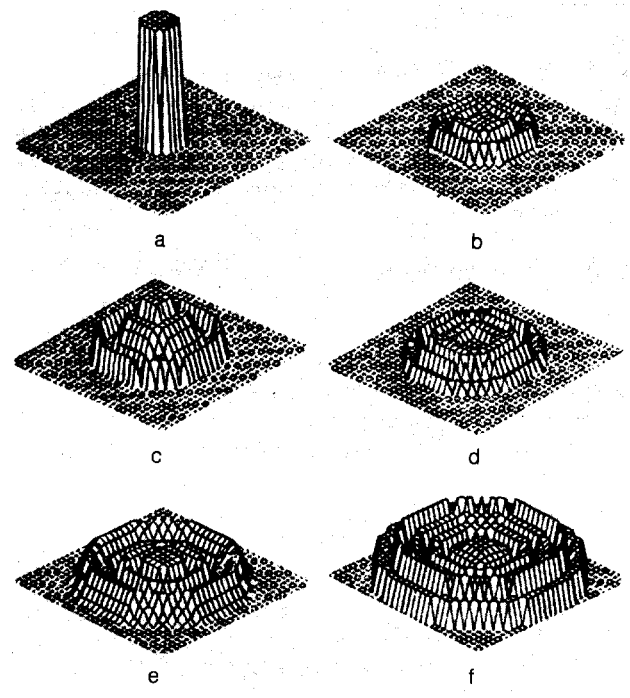

FIG. 30. Spatial evolution of an initially synchronous point population in the case where diffusion coefficient depends on the population count and age of the organism.[224]

(or diffusion constant) on age is different from that which was specified (usually arbitrarily) by Eq. (97). In this case the bacteria remain mobile throughout their entire life, but the maximum mobility of each cell occurs approximately midway through its life.[225,226] The chemotactic response of each individual bacterium also changes.[226] Moreover, the expansion rate of the bacterial chemotaxis rings quickly stabilizes and then remains constant.[169,227] Thus, the time variability of taxis and of mobility of individual cells contrasts sharply with the constancy of the velocity of motion of the cell collectives—population waves.

4. CONCLUSIONS

It might appear that a detailed biophysical investigation of the behavior of individual micro-organisms and their populations is of purely scientific interest and it is difficult to find practical applications from these results. However, this is not so.

As already pointed out at the beginning of the paper (see Table I), many types of fertilizers, vitamins, feed proteins, and antibiotics are the products of micro-organisms. The manufacture of technical devices and entire systems can be a product of biotechnology. The use of micro-organisms together with biomolecular complexes (proteins, enzymes, etc.) will possibly play a distinctive role in the future in the building of biological measuring devices.

Whereas in earlier years the primary problem to be overcome was the reproduction of the operating principles of living systems in engineering, today hybrid systems have already been developed, including metal elements as well as bioelements. The development of biological systems for technical application has begun.[5,232]

It is obvious from what has been said above that a micro-organism is a unique logic module—a "biochip" less than 10 μm in size combining in one "case" a sensor, logic and actuator (or search) mechanisms. Thanks to the development of continuous methods, the growing of micro-organisms is inexpensive, and their resources are essentially unlimited. It is obvious that by understanding the individual and collective life of micro-organisms one can attempt to develop a unique technology for the production of logic computer microdevices from them, based on parametric (chemical or physical) effects, which will stimulate and direct the self-organization process of micro-organisms in microdevices.

It is quite clear (although this is not easily verified formally) that the patterns appearing in microbe populations are open systems, existing far from thermodynamic equilibrium. It is also clear that such systems can maintain their order only when the processes controlling their behavior are essentially nonlinear (see Refs. 10 and 11). In fact, for example, the tumbling frequency, as shown in Refs. 97 and 145, depends nonlinearly on the attractant gradient. This property underlies the nonlinear character of the equations modeling the propagation of the bacterial waves of chemotaxis (see Eqs. (18), (57) and (87)). The mathematical models of gyrotaxis are also highly nonlinear.[198] On the basis of microbiological modules one can attempt to develop analog wave devices, capable of modeling nonlinear processes in systems being developed.

We have seen that as a result of the nonlinear action of the ambient or physical factors on micro-organisms, mobile or immobile spatial patterns appear: population waves (see Figs. 11 and 16), swarming effects (see Fig. 13), Rayleigh–Taylor cells (see Fig. 18), green holes (see Fig. 19), etc. These structurally organized populations of organisms in turn alter the ambient medium in such a manner as to maintain their existence. Thus, the chemotaxis rings induce an attractant concentration gradient, which is a necessary condition for the existence of such rings (see Sect. 3.1). Another example: converging chemotaxis rings form a demarcation zone (see Fig. 21). The drawing off of the culture substrate from it (see Fig. 3) and the possible dependence of the mobility of the bacteria on the substrate concentration contribute to the stabilization of this zone (see Sect. 3.7).

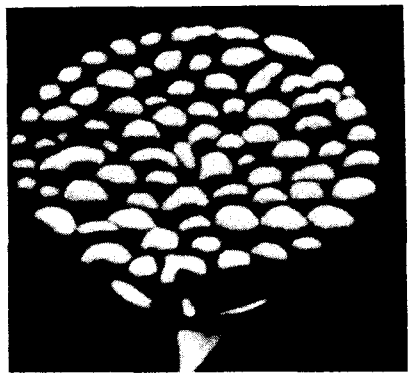

FIG. 31. Cellular structure of a flame.[192]

Thus, the genesis of the population waves and patterns formed by micro-organisms is a result caused by the interaction of the organisms and medium and a transition from a random chaotic motion of the individual cells to a deterministic motion of cell collectives.

Such a transition—from random fluctuations to ordered wave motions and spatial patterns—is characteristic not only of living systems but also of some comparatively simple physical-chemical processes (the classical example is the formation of the cellular flame; Ref. 39; Fig. 31). An investigation of analogies between nonliving and living systems can be of no small interest to researchers.

As already pointed out, micro-organisms are able to convert energy of very different forms: chemical, light, mechanical, magnetic. They provide for the detection of a wide spectrum of substances and in a number of cases they are characterized by high sensitivity ($\sim 10^{-6}$ M concentration of the substances being detected[96]). By means of them it may be possible to detect microimpurities of ions and complex molecules in water and in multicomponent liquids. A measuring system describable as a "bacterium on an optical leash" can be based on the system already described by Berg (see Fig. 3).

Bioengineering, established on a base of organic materials including micro-organisms, is taking its first steps, but it will not be surprising if in the very near future it comes into widespread use together with traditional technical microsystems. One of the goals of this review is to attract attention—especially of young researchers—to this area of science, which lies at the interface of physics, biophysics, biochemistry and engineering.

[1] I. Prigogine, *From Being to Becoming: Time and Complexity in the Physical Sciences*, Freeman, San Francisco (1980).

[2] G. R. Ivanitskiĭ, N. G. Esipova, R. A. Abagyan, and S. E. Shnol', Biofiz. **30**, 418 (1985).
[3] R. B. Khesin, *Genome Variability*, Nauka, Moscow, 1985.
[4] G. R. Ivanitskiĭ, *Growth Rhythms of Complex Systems*, Znanie, Moscow, 1989 (Ser. "Cybernetics, Mathematics", No. 9).
[5] *Bioengineering—A New Direction of Computerization*, Nauka, Moscow, 1990.
[6] Yu. A. Ovchinnikov and G. R. Ivanitskiĭ, Vestn. Akad. Nauk SSSR No. 7, 32 (1982).
[7] H. C. Berg, Rev. Sci. Instrum. **42**, 868 (1971).
[8] H. C. Berg, Sci. Am. **233**, No. 1, 36 (1975).
[9] M. A. Tsyganov, A. B. Medvinskiĭ, V. M. Ponomarev, and G. R. Ivanitskiĭ, Dokl. Akad. Nauk SSSR **306**, 731 (1989).
[10] M. V. Vol'kenshteĭn, *Biophysics*, Nauka, Moscow, 1981.
[11] G. Nicolis and I. Prigogine, *Self-Organization in Nonequilibrium Systems*, Wiley, New York, 1977.
[12] A. Franklin, Am. J. Phys. **44**, 527 (1976).
[13] E. M. Purcell, Am. J. Phys. **45**, 3 (1977).
[14] H. C. Berg and D. A. Brown, *Nature* (London) **239**, 500 (1972).
[15] T. N. Belyakova, A. N. Glagolev, and V. P. Skulachev, Biokhimiya **41**, 1478 (1976).
[16] A. N. Glagolev and V. P. Skulachev, *Nature* (London) **272**, 280 (1978).
[17] S. H. Larsen, J. Adler, J. J. Gargus, and R. W. Hogg, Proc. Nat. Acad. Sci. USA **71**, 1239 (1974).
[18] M. D. Manson, P. Tedesco, H. C. Berg, F. M. Harold, and C. van der Drift, Proc. Nat. Acad. Sci. USA **74**, 3060 (1977).
[19] P. Matsumura, M. Silverman, and M. Simon, J. Bacteriol. **132**, 996 (1977).
[20] J. I. Shioi, J. Imae, and F. Oosawa, *ibid.* **133**, 1083 (1978).
[21] H. G. Shlegel, *General Microbiology*, Cambridge Univ. Press (1986).
[22] M. L. DePamphilis and J. Adler, J. Bacteriol. **105**, 376 (1971).
[23] M. L. DePamphilis and J. Adler, *ibid.* 384.
[24] M. L. DePamphilis and J. Adler, *ibid.* 396.
[25] A. M. Lawn, J. Gen. Microbiol. **101**, 111 (1977).
[26] M. W. McDonough, J. Mol. Biol. **12**, 342 (1965).
[27] B. F. Poglazov, A. L. Metlina, and V. V. Novikov, Izv. Akad. Nauk SSSR Ser. Biol. No. 5, 672 (1981).
[28] W. Bode and A. Blume, FEBS Lett. **36**, 318 (1973).
[29] B. R. Gerber, S. Asakura, and F. Oosawa, J. Mol. Biol. **74**, 467 (1973).
[30] H. C. Berg, *Nature* (London) **249**, 77 (1974).
[31] M. D. Manson, P. M. Tedesco, and H. C. Berg, J. Mol. Biol. **138**, 541 (1980).
[32] F. Cohn, Beitr. Biol. Pflanz **1**, 127 (1875).
[33] T. W. Engelmann, Pflugers Arch. Jesamte Physiol. Menschen Tiere **25**, 285 (1881).
[34] T. W. Engelmann, *ibid.* **26**, 537.
[35] T. W. Engelmann, *ibid.* **30**, 95 (1883).
[36] W. Pfeffer, Unters. Bot. Inst. Tubingen **1**, 363 (1884).
[37] R. M. Macnab, Trends Biochem. Sci. **4**, 10 (1979).
[38] H. C. Berg, *Nature* (London) **254**, 389 (1975).
[39] A. G. Merzhanov and É. N. Rumanov, Usp. Fiz. Nauk **151**, 553 (1987) [Sov. Phys. Usp. **30**, 293 (1987)].
[40] J. G. Shoesmith, J. Gen. Microbiol. **22**, 528 (1960).
[41] W. R. Schneider and R. N. Doetsch, J. Bacteriol. **117**, 696 (1974).
[42] K. E. Schreiner, J. Biomech. **4**, 73 (1971).
[43] M. E. J. Holwill and R. E. Burge, Arch. Biochem. Biophys. **101**, 249 (1963).
[44] C. J. Coakley and M. E. J. Holwill, J. Theor. Biol. **35**, 525 (1972).
[45] M. E. J. Holwill and C. A. Miles, Biophys. J. **11**, 851 (1971).
[46] K. E. Machin, J. Exp. Biol. **35**, 796 (1958).
[47] R. M. Macnab, *Escherichia coli and Salmonella typhimurium. Cellular and Molecular Biology*, ed. F. C. Neidhardt, American Society for Microbiology, Washington (1981), Vol. 1, p. 732.
[48] S. H. Larsen, R. W. Reader, E. N. Kort, W. W. Tso, and J. Adler, Nature (London) **249**, 74 (1974).
[49] B. I. Taylor and D. E. Koshland, Jr., J. Bacteriol. **119**, 640 (1974).
[50] H. C. Berg, Ann. Rev. Biophys. Bioeng. **4**, 119 (1975).
[51] A. N. Glagolev, Usp. Mikrobiol. **18**, 163 (1983).
[52] N. R. Krieg, Bacteriol. Rev. **40**, 55 (1976).
[53] A. T. Chwang and T. Y. Wu, Proc. R. Soc. London Ser. B **178**, 327 (1971).
[54] A. Ishihara, J. E. Segall, S. M. Block, and H. C. Berg, J. Bacteriol. **155**, 228 (1983).
[55] R. M. Macnab and D. P. Han, Cell **32**, 109 (1983).
[56] N. Tsang, R. M. Macnab, and D. E. Koshland, Jr., Science **181**, 60 (1973).
[57] R. M. Macnab and D. E. Koshland, Jr., Proc. Natl. Acad. Sci. USA **69**, 2509 (1972).
[58] D. E. Koshland, Jr., FEBS Lett. **40**, 53 (1974).
[59] J. Adler, Science **166**, 1588 (1969).
[60] J. Adler, G. L. Hazelbauer, and M. M. Dahl, J. Bacteriol. **115**, 824 (1973).
[61] R. E. Mesibov and J. Adler, *ibid.* **112**, 315 (1972).
[62] G. L. Hazelbauer, R. E. Mesibov, and J. Adler, Proc. Natl. Acad. Sci. USA **64**, 1300 (1969).
[63] J. Adler, *Primitive Sensory and Communication Systems; The Taxes and Tropisms of Micro-Organisms and Cells*, M. J. Carlile (ed.), Academic Press, London, (1975), p. 92.
[64] W. W. Tso and J. Adler, J. Bacteriol. **118**, 560 (1974).
[65] R. M. Macnab and D. E. Koshland, Jr., J. Mol. Biol. **84**, 399 (1974).
[66] B. L. Taylor and D. E. Koshland, Jr., J. Bacteriol. **123**, 557 (1975).
[67] B. L. Taylor, J. B. Miller, H. M. Warrick, and D. E. Koshland, Jr., *ibid.* **140**, 567 (1979).
[68] M. J. Carlile, Ref. 63, p. 1.
[69] F. Lenci and G. Colombetti, Ann. Rev. Biophys. Bioeng. **7**, 341 (1978).
[70] W. Nultsch, Ref. 63, p. 30.
[71] J. Adler, J. Gen. Microbiol. **74**, 77 (1973).
[72] Y. Imae, T. Mizuno, and K. Maeda, J. Bacteriol. **159**, 368 (1984).
[73] K. Maeda, Y. Imae, J.-I. Shioi, and F. Oosawa, *ibid.* **127**, 1039 (1976).
[74] Y. Imae, *Sensing and Response in Micro-Organisms*, M. Eisenbach and M. Balaban (eds.), Elsevier, Amsterdam (1985), p. 73.
[75] J. Ingraham, Ref. 47, p. 1543.
[76] J. B. Miller and D. E. Koshland, Jr., J. Mol. Biol. **111**, 183 (1977).
[77] R. B. Frankel and R. B. Blakmore, Bioelectromagn. **10**, 223 (1989).
[78] R. Eckert, Science **176**, 473 (1972).
[79] M. Eisenbach, J. R. Zimmerman, A. Ciobotariu, H. Fischler, and R. Korenstein, Bioelectrochem. Bioenergy **10**, 499 (1983).
[80] M. S. Plesset, C. G. Whipple, and H. Winet, J. Theor. Biol. **59**, 331 (1976).
[81] M. S. Plesset and H. Winet, *Nature* (London) **248**, 441 (1974).
[82] J. O. Kessler, Commun. Theor. Biol. **1**, 85 (1989).
[83] B. L. Taylor and D. E. Koshland, Jr., J. Supramol. Struct. **4**, 343 (1976).
[84] D. E. Koshland, Jr., Physiol. Rev. **59**, 811 (1979).
[85] J. Adler, J. Supramol. Struct. **4**, 305 (1976).
[86] A. F. Russo and D. E. Koshland, Jr., Science **220**, 1016 (1983).
[87] A. F. Russo and D. E. Koshland, Jr., Ref. 74, p. 27.
[88] P. G. Strange and D. E. Koshland, Jr., Proc. Natl. Acad. Sci. USA **73**, 762 (1976).
[89] R. S. Zukin and D. E. Koshland, Jr., Science **193**, 405 (1976).
[90] R. S. Zukin, Biochem. **18**, 2139 (1979).
[91] J. Adler, Ann. Rev. Biochem, **44**, 341 (1975).
[92] D. E. Koshland, Jr., *Advances in Neurochemistry*, B. W. Agranoff and M. H. Aprison (eds.) Plenum Press, New York, 1977, Vol. 2, p. 277.
[93] N. R. Tsang, R. Macnab, and D. E. Koshland, Jr., Science **181**, 60 (1973).
[94] J. Lederberg, Genetics **41**, 845 (1956).
[95] F. W. Dahlquist, R. A. Elwell, and P. S. Lovely, J. Supramol. Struct. **4**, 329 (1976).
[96] D. A. Brown and H. C. Berg, Proc. Natl. Acad. Sci. USA **71**, 1388 (1974).
[97] H. C. Berg and E. M. Purcell, Biophys. J. **20**, 193 (1977).
[98] R. Mesibov, G. W. Ordal, and J. Adler, J. Gen. Physiol. **62**, 203 (1973).
[99] D. E. Thomsen, Sci. News **125**, 298 (1984).
[100] G. L. Hazelbauer, *Nature* (London) **279**, 18 (1979).
[101] G. W. Ordal, Bioscience, **30**, 408 (1980).
[102] M. S. Springer, M. F. Goy, and J. Adler, Nature (London) **280**, 279 (1979).
[103] M. S. Springer, M. F. Goy, and J. Adler, Proc. Natl. Acad. Sci. USA **74**, 183 (1977).
[104] J. Adler, Ref. 74, p. 9.
[105] S. Khan, R. M. Macnab, A. L. De Franco, and D. E. Koshland, Jr., Proc. Natl. Acad. Sci. USA **75**, 4150 (1978).
[106] M. F. Goy, M. S. Springer, and J. Adler, Cell **15**, 1231 (1978).
[107] M. F. Goy, M. S. Springer, and J. Adler, Proc. Natl. Acad. Sci. USA **74**, 4964 (1977).
[108] D. E. Koshland, Jr., Science **196**, 1055 (1977).
[109] W. Feller, *An Introduction to Probability Theory and its Applications*, Wiley, New York, 1950.
[110] S. M. Block, J. E. Segall, and H. C. Berg, J. Bacteriol. **154**, 312 (1983).
[111] M. Delbruck and W. Reichardt, *Cellular Mechanisms in Differentiation and Growth*, D. Rudnick (ed.), Princeton University Press, Princeton, 1956, p. 3.
[112] S. E. Luria and R. Latarjet, J. Bacteriol. **53**, 149 (1947).
[113] A. L. Koch, Ref. 47, Vol. 2, p. 1606.
[114] J. L. Spudich and D. E. Koshland, Jr., *Nature* (London), **262**, 467 (1976).
[115] C. R. Woese and G. E. Fox, Proc. Natl. Acad. Sci. USA **74**, 5088 (1977).
[116] J. Adler, Sci. Am. **234**, 40 (1976).

[117] J. W. Lengeler, La Recherche **21**, 20 (1990).
[118] J. Adler, J. Bacteriol. **92**, 121 (1966).
[119] J. Adler, Science **153**, 708 (1966).
[120] J. Adler and M. M. Dahl, J. Gen. Microbiol. **46**, 161 (1967).
[121] J. Adler and B. Templeton, *ibid.* 175.
[122] E. F. Keller and L. A. Segel, J. Theor. Biol. **30**, 225 (1971).
[123] E. F. Keller and L. A. Segel, *ibid.* 235.
[124] S. Chandrasekhar, Rev. Mod. Phys. **15**, 57 (1943).
[125] E. F. Keller and L. A. Segel, J. Theor. Biol. **26**, 399 (1970).
[126] M. McCabe and T. V. Laurent, Biochem. Biophys. Acta **399**, 131 (1975).
[127] M. Holz and S.-H. Chen, Biophys. J. **26**, 243 (1979).
[128] S. C. Peterson and P. B. Noble, *ibid.* **12**, 1048 (1972).
[129] S. H. Zigmond, *Nature* (London) **249**, 450 (1974).
[130] R. Nossal and S. H. Zigmond, Biophys. J. **16**, 1171 (1976).
[131] R. L. Hall and S. C. Peterson, *ibid.* **25**, 365 (1979).
[132] R. L. Hall, J. Math. Biol. **4**, 327 (1977).
[133] T. M. Konijn, Ref. 68, p. 101.
[134] V. Nanjundiah, J. Theor. Biol. **42**, 63 (1973).
[135] A. D. J. Robertson and J. F. Grutsch, Cell **24**, 603 (1981).
[136] V. Nanjundiah, Proc. Ind. Acad. Sci. Animal Sci. **94**, 639 (1985).
[137] M. Gail and C. W. Boone, Biophys. J. **10**, 980 (1970).
[138] W. Bredt, K. H. Hofling, H. H. Heunert, and S. Milthaler, Z. Med. Mikrobiol. Immunol. **156**, 39 (1970).
[139] R. Nossal and G. H. Weiss, J. Theor. Biol. **47**, 103 (1974).
[140] R. Nossal and G. H. Weiss, J. Stat. Phys. **10**, 245 (1974).
[141] R. Nossal, *Biological Growth and Spread*, W. Jager, H. Rost, and P. Tautu (eds.), Springer-Verlag, Berlin, (1980), p. 410 (*Lecture Notes in Biomathematics*, Vol. 38).
[142] P. S. Lovely and F. W. Dahlquist, J. Theor. Biol. **50**, 477 (1975).
[143] L. Yu. Zaval'skiĭ, D. E. Svetogorov, V. N. Brezgunov, and V. G. Popov, Dokl. Akad. Nauk SSSR **279**, 488 (1984).
[144] L. Yu. Zaval'skiĭ, D. E. Svetogorov, and V. N. Brezgunov, Biofiz. **30**, 93 (1985).
[145] L. Yu. Zaval'skiĭ, Biofiz. **33**, 328 (1988).
[146] L. A. Segel and J. L. Jackson, J. Mechanochem. Cell Motil. **2**, 25 (1973).
[147] G. Hauser, *Über Fäulnisbakterien und deren Beiziehungen zur Septicaemia*, Vogel, Leipzig (1885).
[148] R. H. Schwarzhoff, *The Role of Chemotaxis in the Swarming of Proteus mirabilis*, Iowa State University (1974).
[149] F. J. M. Hoeniger, J. Gen. Microbiol. **40**, 29 (1965).
[150] F. D. Williams and R. H. Schwarzhoff, Ann. Rev. Microbiol. **32**, 101 (1978).
[151] I. Lominski and A. C. Lendrum, J. Pathol. Bacteriol. **59**, 688 (1947).
[152] O. Moltke, *Contributions to the Characterization and Systematic Classification of Bac. Proteus vulgaris* (Hauser), Levin and Munksgaard, Copenhagen (1927).
[153] F. D. Williams, D. M. Anderson, P. S. Hoffman, R. H. Schwarzhoff, and S. Leonard, J. Bacteriol. **127**, 237 (1976).
[154] V. G. Babskiĭ, *Thermodynamics of Irreversible Processes*, Nauka, Moscow (1987), p. 146.
[155] *Micro-Organisms in Space Flight*, K. M. Sytnik (ed.), Naukova Dumka, Kiev (1983).
[156] Yu. M. Romanovskiĭ, N. V. Stepanova, and D. S. Chernavskiĭ, *Mathematical Biophysics*, Nauka, Moscow (1984).
[157] B. N. Belintsev, Usp. Fiz. Nauk **141**, 55 (1983) [Sov. Phys. Usp. **26**, 775 (1983)].
[158] L. V. Belousov, *The Problem of Embryonic Formation*, Moscow State University, Moscow (1971).
[159] A. M. Zhabotinskiĭ, *Nonlinear Waves. Self-Organization*, Nauka, Moscow (1983), p. 16.
[160] M. M. Frank-Kamenetskiĭ, *Diffusion and Heat Transfer in Chemical Kinetics*, Nauka, Moscow (1987).
[161] V. A. Vasil'ev, Yu. M. Romanovskiĭ, and V. G. Yakhno, Usp. Fiz. Nauk **128**, 625 (1979) [Sov. Phys. Usp. **22**, 615 (1979)].
[162] G. R. Ivanitskiĭ, V. I. Krinskiĭ, and E. E. Sel'kov, *Mathematical Biophysics of Cells*, Nauka, Moscow (1978).
[163] V. I. Krinskiĭ, Vestn. Akad. Nauk SSSR No. 1, 6 (1980).
[164] V. I. Krinskiĭ and A. M. Zhabotinskiĭ, *Autowave Processes in Systems with Diffusion*, Institute of Applied Physics, Academy of Sciences of the USSR, Gorky (1981), p. 6.
[165] V. I. Krinskiĭ, A. B. Medvinskiĭ, and A. V. Panfilov, *Evolution of Autowave Vortices (Waves in the Heart)*, Znanie, Moscow (1986).
[166] V. I. Krinskiĭ and A. S. Mikhaĭlov, *Autowaves*, Znanie, Moscow (1984).
[167] L. S. Polak and A. S. Mikhaĭlov, *Self-Organization in Nonequilibrium Physicochemical Systems*, Nauka Press, Moscow, 1983.
[168] M. Dworkin, *Microbiological Differentiation*, Cambridge University Press (1973), p. 125.
[169] A. B. Medvinskiĭ, M. A. Tsyganov, I. L. Fishov, V. A. Karpov, V. M. Ponomareva, and G. R. Ivanitskiĭ, Dokl. Akad. Nauk SSSR **314**, 1495 (1990).
[170] M. Sussman, *Developmental Biology*, Prentice-Hall, Englewood Cliffs New Jersey (1973).
[171] R. P. Blakmore, Science, **190**, 377 (1975).
[172] R. P. Blakmore and R. B. Frankel, Sci. Am. **245**, 42 (1981).
[173] R. P. Blakmore, Ann. Rev. Microbiol. **36**, 217 (1982).
[174] D. Balkwill, D. Maratea, and R. P. Blakmore, J. Bacteriol. **141**, 1399 (1980).
[175] K. M. Towe and T. T. Moench, Earth Planetary Sci. Lett. **52**, 213 (1981).
[176] Y. A. Gorby, T. J. Beveridge, and R. P. Blakmore, J. Bacteriol. **170**, 834 (1988).
[177] R. B. Frankel, G. G. Papaefthymion, R. P. Blakmore, and W. D. O'Brien, Biochem. Biophys. Acta **763**, 147 (1983).
[178] S. Mann, R. B. Frankel, and R. P. Blakmore, *Nature* (London) **310**, 405 (1984).
[179] R. B. Frankel and R. P. Blakmore, J. Magn. Magn. Mater. **15–18**, 1562 (1980).
[180] A. J. Kalmijn, IEEE Trans. Magn. **MAG-17**, 1113 (1981).
[181] B. D. Teague, M. Gilson, and A. J. Kalmijn, Biol. Bull. **157**, 399 (1979).
[182] A. M. Spormann, FEMS Microbiol. Ecol. **45**, 37 (1987).
[183] M. Carlile, A. W. L. Dudeney, B. K. Hebenstreit, and R. H. Heerema, J. Magn. Magn. Mater. **67**, 291 (1987).
[184] D. C. Guell, H. Brenner, R. B. Frankel, and H. Hartman, J. Theor. Biol. **135**, 525 (1988).
[185] H. Wager, Proc. R. Soc. London Ser. B **83**, 94 (1911).
[186] E. C. Teodoresco and E. Angelesco, Kolloid. Z. **97**, 216 (1941).
[187] J. B. Loefer and R. B. Mefferd, Jr., Am. Nat. **86**, 325 (1952).
[188] N. J. Robbins, Bull. Torrey Bot. Club **79**, 107 (1952).
[189] J. R. Platt, Science **133**, 1766 (1961).
[190] S. L. Gittleson and T. L. Jahn, Exp. Cell Res. **51**, 579 (1968).
[191] E. M. Shvirst, V. I. Krinskiĭ, and G. R. Ivanitskiĭ, Biofiz. **29**, 649 (1984).
[192] B. Lewis and G. von Elbe, *Combustion, Flames and Explosions of Gases*, Academic Press, New York (1961).
[193] Rayleigh, Proc. London Math. Soc. **14**, 170 (1883).
[194] M. S. Plesset and C. G. Whipple, Phys. Fluids **17**, 1 (1974).
[195] A. M. Roberts, *Swimming and Flying*, J. T. Wu *et al.* (eds.), Plenum Press, New York, 1975, Vol. 1, p. 377.
[196] J. O. Kessler, *Nature* (London) **313**, 218 (1985).
[197] J. Happel and H. Brenner, *Low Reynolds Number Hydrodynamics*, Prentice-Hall, New York, 1965.
[198] J. O. Kessler, J. Fluid Mech. **173**, 191 (1986).
[199] W. S. Childress, M. Levandowsky, and E. A. Spiegel, *ibid.* **63**, 591 (1975).
[200] J. O. Kessler, Contemp. Phys. **26**, 147 (1985).
[201] T. J. Pedley, N. A. Hill, and J. O. Kessler, J. Fluid Mech. **195**, 223 (1988).
[202] G. Rosen, Math. Biosci. **24**, 17 (1975).
[203] G. R. Ivanitskiĭ, V. I. Krinskiĭ, M. A. Tsyganov, and K. I. Agladze, Biofiz. **33**, 372 (1988).
[204] E. O. Budrene, Dokl. Akad. Nauk SSSR **283**, 470 (1985).
[205] E. O. Budrene, Biofiz. **33**, 373 (1988).
[206] V. Yu. Shakhbazyan, A. B. Medvinskiĭ, K. I. Agladze, M. A. Tsyganov, and G. R. Ivanitskiĭ, Dokl. Akad. Nauk SSSR **310**, 737 (1990).
[207] R. Lapidus and R. Schiller, Biophys. J. **22**, 1 (1978).
[208] G. Rosen, Bull. Math. Biol. **45**, 837 (1983).
[209] A. B. Medvinsky, M. A. Tsyganov, V. Yu. Shakhbazian, V. M. Ponomareva, and G. R. Ivanitsky, 10th International Biophysics Congress, Vancouver, 1990, p. 445.
[210] S. Luria, D. Darnell, D. Baltimore, and E. Campbell, *General Virology*, Wiley, New York (1975).
[211] P. Demerec and H. Fano, Genetics **30**, 119 (1945).
[212] M. H. Adams and B. H. Park, Virology **2**, 719 (1965).
[213] G. R. Ivanitsky, A. S. Kunisky, and M. A. Tsyganov, *Self-Organization: Autowaves and Structures Far from Equilibrium*, V. I. Krinsky (ed.), Springer-Verlag, Berlin, (1984), p. 214.
[214] M. A. Tsyganov and G. R. Ivanitsky, Ref. 209, p. 538.
[215] T. I. Pis'man, T. V. Elkina, M. I. Teremova, N. S. Pechurkin, and I. A. Terskov, Dokl. Akad. Nauk SSSR **241**, 955 (1978).
[216] A. B. Medvinsky, I. L. Fishov, M. A. Tsyganov, and G. R. Ivanitsky, Ref. 209, p. 537.
[217] A. B. Medvinskiĭ, I. L. Fishov, M. A. Tsyganov, and G. R. Ivanitskiĭ, Dokl. Akad. Nauk SSSR **311**, 1479 (1990).
[218] A. S. Tikhonenko, *Ultrastructure of Bacteria Viruses*, Nauka, Moscow (1968).
[219] R. Merle, *Les Hommes proteges*, Editions Gallimard, Paris (1974).
[220] G. W. Salt, *Biological Competition Mechanisms*, Mir Press, Moscow (1964) p. 124 (transl. into Russian).

[221] C. R. Kennedy, Ecological Animal Parasitology, Blackwell Scientific Publications, Oxford (1975).
[222] M. Bezděk and J. Säska, Folia Microbiol. **17**, 366 (1972).
[223] A. Schimz and E. Hildebrand, Nature (London), **317**, 641 (1985).
[224] G. R. Ivanitskiĭ, A. V. Panfilov, and M. A. Tsyganov, Biofiz. **32**, 354 (1987).
[225] A. B. Medvinskiĭ, I. L. Fishov, V. A. Karpov, I. N. Milonova, M. A. Tsyganov, and G. R. Ivanitskiĭ, Dokl. Akad. Nauk SSSR (1991).
[226] I. L. Fishov, A. B. Medvinsky, V. A. Karpov, V. A. Tsyganov, and G. R. Ivanitsky, *Nature* (submitted).
[227] A. J. Wolfe and H. C. Berg, Proc. Natl. Acad. Sci. USA **86**, 6973 (1989).
[228] I. R. Lapidus, J. Theor. Biol. **86**, 91 (1980).
[229] D. Lauffenburger, C. R. Kennedy, and R. Aris, Bull. Math. Biol. **46**, 19 (1984).
[230] D. Lauffenburger, R. Aris, and K. Keller, Biophys. J. **40**, 209 (1982).
[231] T. L. Scribner, L. A. Segel, and E. H. Rogers, J. Theor. Biol. **46**, 189 (1974).
[232] G. R. Ivanitskiĭ, Vestn. Akad. Nauk SSSR No. 3, 118 (1984).

Translated by Eugene R. Heath